Projecting future climate change: Implications of carbon cycle model intercomparisons

Haroon S. Kheshgi
Corporate Strategic Research, ExxonMobil Research and Engineering Company, Annandale, New Jersey, USA

Atul K. Jain
Department of Atmospheric Sciences, University of Illinois, Urbana, Illinois, USA

Received 28 November 2001; revised 20 December 2002; accepted 6 February 2003; published 15 May 2003.

[1] The range of responses of alternate detailed models for the ocean and biosphere components of the global carbon cycle, cataloged in model intercomparison studies, are simulated by a reduced form Earth system model employing a range of model parameters. The reduced form model, parameterized in this way, allows the integration of these components of the carbon cycle with an energy balance climate model with a prescribed range of climate sensitivity. We use this model to construct ranges of: (1) past carbon budgets given past CO_2 concentrations, fossil carbon emissions, and temperature records, (2) future CO_2 concentrations and temperature for given emission scenarios, and (3) CO_2 emissions and temperature for given trajectories of future CO_2 concentrations leading to constant levels within the next several centuries. Carbon cycle is an additional contributor to uncertainty in climate projections that is calculated to expand the range of projected global temperature beyond that reported in the 2001 Intergovernmental Panel on Climate Change assessment. *INDEX TERMS:* 1620 Global Change: Climate dynamics (3309); 1615 Global Change: Biogeochemical processes (4805); 4806 Oceanography: Biological and Chemical: Carbon cycling

Citation: Kheshgi, H. S., and A. K. Jain, Projecting future climate change: Implications of carbon cycle model intercomparisons, *Global Biogeochem. Cycles*, *17*(2), 1047, doi:10.1029/2001GB001842, 2003.

1. Introduction

[2] The global carbon cycle is one link in a causal chain linking human activities to changes in climate. The causal chain includes relations between human activities, atmospheric emissions, alteration of components of the climate system (greenhouse gas concentration, aerosols, land cover, etc.), changes in the radiative balance of the atmosphere, and the response of climate. The behavior of global carbon cycle determines the response of the atmospheric concentration of CO_2, the greenhouse gas of greatest concern, to sources and sinks of CO_2 from a wide range of human activities, particularly CO_2 emissions from fossil fuel consumption. Currently, our ability to forecast future climate is in question. Models are used to make projections of future climate, based on scenarios of future human activities and emissions, by simulating each link in the causal chain relating these scenarios to changes in climate. The estimation of the uncertainty of this causal chain remains an important scientific challenge.

[3] The global carbon cycle, the link relating emissions of CO_2 to its concentration is often "assumed" to lead to relatively certain predictions of its behavior given the clear trend in the concentration of CO_2 and the clear attribution of the anthropogenic cause of this trend. Climate projections [*Cubasch et al.*, 2001] communicated by the Intergovernmental Panel on Climate Change (IPCC) in its Third Assessment Report (TAR) did not account for uncertainty in future carbon cycle behavior. Uncertainty in carbon cycle behavior was, however, assessed in the reported IPCC CO_2 projections [*Prentice et al.*, 2001], and carbon cycle model intercomparison was one approach used to make this assessment: details of this approach are given in this paper. A range of global carbon cycle response is exhibited by current detailed carbon cycle models resulting in a range of projected CO_2 concentration, given a scenario for emissions; this range is wider than had been considered in previous assessments and contrary to the common assumption. Consequently, when accounted for in the simulation of the entire climate system, the range of climate projections also becomes somewhat wider.

[4] Many types of models have been used to simulate carbon cycle on different spatial and temporal scales. For the assessment of the effects of anthropogenic emissions on climate, the global scale is of interest and timescales spanning decades to centuries are relevant. Methods are needed to characterize the uncertainty of such projections at these scales, even though the result may be ambiguous. A challenge for global carbon cycle models is to forecast the response of ocean, plant, and soil carbon uptake under conditions unprecedented in history. The limited opportu-

0886-6236/03/2001GB001842$12.00

nities to validate such models by comparison to data, therefore only arise under conditions or scales different than an assessment model's task.

[5] Approaches that have been used to provide information about the uncertainty of projections have included model sensitivity analysis, model calibration, and model intercomparison. Model sensitivity can be used to assess uncertainty if the model structure is accurate and if there is sufficient information about model parameters. For example, *Joos et al.* [2001] made bounding assumptions on the ranges of some parameters of their climate/carbon system model to produce a bounding range of CO_2 concentration projections; in this way a study of model sensitivity was used in the IPCC TAR [*Prentice et al.*, 2001] as an indicator of uncertainty in projections. Model calibration can be used to estimate model parameters provided the model structure is correct and data are available with which to calibrate the model. In the IPCC Special Report on Radiative Forcing (SRRF) [*Schimel et al.*, 1995] and the Second Assessment Report (SAR) [*Schimel et al.*, 1996], ocean tracer data along with model intercomparisons were used to calibrate global carbon cycle models to give bounds on CO_2 projections. Of course, both approaches can be combined by Bayesian parameter estimation applying prior information about model parameters as well as observation-based constraints [cf. *Kheshgi et al.*, 1999; *Kheshgi and Jain*, 2000]. Parameter estimation, however, might not give reliable results if the correct model structure is not known.

[6] Model intercomparisons can provide some information about plausible model structures as well as providing information about the uncertainty of projections. If model results cannot be rejected based on, e.g., comparisons to data, then the envelope of model results must be contained within the uncertainty range, thereby, forming a lower bound on the uncertainty range. In this study, we make new reconstructions of past carbon budgets, projections of CO_2 concentration and temperature for given scenarios of future emissions, and estimate implications of concentration stabilization on CO_2 emissions and temperature. The range of CO_2 concentration projections detailed here were also used in the IPCC TAR [*Prentice et al.*, 2001], however, the associated climate projections were not shown in the IPCC TAR.

[7] In this study, we use a globally aggregated climate/carbon cycle model to represent the globally aggregated responses of detailed models for the ocean and terrestrial biosphere components of the Earth system that have been cataloged in model intercomparison studies [*Cramer et al.*, 2001; *Orr et al.*, 2001; *Prentice et al.*, 2001]. In section 2, the model is described along with its calibration to the results of model intercomparisons. In section 3, the modeled response of past global carbon cycle is reconstructed and modeled past carbon budgets are compared to budgets based on observational constraints. In addition, specification of observed past climate introduces an adjustment of the carbon budgets based on carbon cycle models over the past decades not included in past assessments. In section 4, future projections of CO_2 and global temperature are made driven by emission scenarios, and including the range of model parameters calibrated to reproduce model intercomparison results. Ranges of CO_2 projections presented here, and in the IPCC TAR, are wider than presented in past IPCC assessments. And ranges of projected global mean temperatures presented here are wider than presented in the IPCC TAR in which uncertainty in carbon cycle response was not accounted for in ranges of climate projections. Finally, projections beyond a century in duration leading to constant levels of CO_2 concentration show the increasing importance, with time in this model simulation, of the ocean carbon sink relative to that of the terrestrial biosphere.

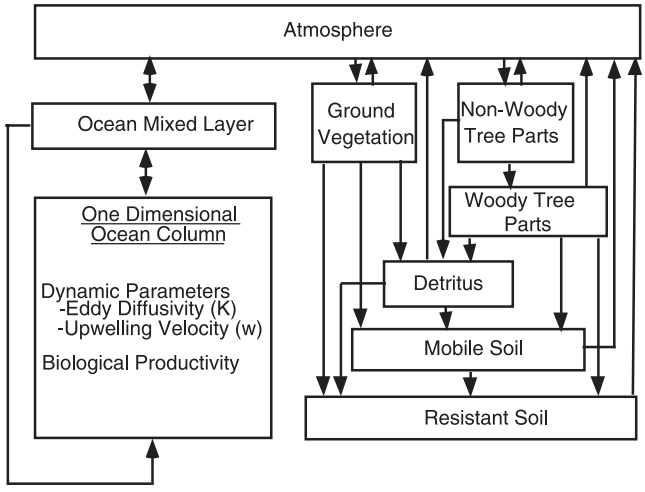

Figure 1. Schematic diagram of the ISAM coupled atmosphere-ocean-biosphere model for the global carbon cycle.

2. Methodology

2.1. The Reduced Form Carbon/Climate System Model ISAM

[8] The Earth system exhibits interactions between carbon cycle and climate, as well as effects of human activities through fossil CO_2 emissions, land use, and other alterations of the environment. A variety of detailed models for climate and components of the carbon cycle have been developed. In addition, detailed models are being coupled to approximate the Earth system in increasing detail, but only for select detailed component models. To approximate the behavior of combinations of many detailed component models, we use the globally aggregated (i.e., reduced form) Earth system model, the Integrated Science Assessment Model (ISAM) [*Jain et al.*, 1994; *Jain and Hayhoe*, 2003].

[9] The global carbon cycle component of ISAM depicted in Figure 1 is used to simulate the exchange of carbon dioxide between the atmosphere, reservoirs of carbon in the terrestrial biosphere, and the ocean column and mixed layer [*Jain et al.*, 1994, 1995, 1996; *Kheshgi et al.*, 1996, 1999]. The model consists of a homogeneous atmosphere, an ocean mixed layer and land biosphere boxes, and a vertically resolved upwelling-diffusion deep ocean. The detailed description of the ocean and land-biosphere components of this model are given by *Jain et al.* [1995] and *Kheshgi et*

al. [1996], respectively, and a discussion of model parameters by *Kheshgi et al.* [1999].

[10] To estimate terrestrial biospheric fluxes, a six-box globally aggregated terrestrial biosphere submodel is coupled to the atmosphere box (Figure 1). The six boxes represent ground vegetation, nonwoody tree parts, woody tree parts, detritus, mobile soil, and resistant soil. The mass of carbon contained in the different reservoirs and their turnover times as well as the rates of exchange between them have been based on the analysis by *Harvey* [1989a] and *Kheshgi et al.* [1996]. The effects of land use are included by changing (decreasing with time) the total productive land area covered by the terrestrial biosphere. The carbon mass in each of the boxes is proportional to the total productive land area. A simple model representation of biospheric response to changes in the atmospheric concentration of CO_2 and the global mean annual near-surface temperature over land are included. An increase in the rate of net photosynthesis of trees or net primary productivity (NPP) of ground vegetation, relative to preindustrial times, is modeled to be proportional to the logarithm of the relative increase in atmospheric CO_2 concentration from its preindustrial value. The magnitude of the modeled biospheric sink depends primarily on the chosen value of the proportionality constant β, the CO_2 fertilization factor [*Keeling*, 1973; *Harvey*, 1989b; *Wigley*, 1993]. Exchange of carbon to and from terrestrial biosphere boxes (respiration, translocation, and photosynthesis) vary with global mean annual temperature according to a Q_{10} formulation, i.e., where net primary production, translocation, and respiration rates are proportional to $(Q_{10})^{T/10^{\circ}C}$, where T is the global mean land temperature and Q_{10} is a model parameter [*Harvey*, 1989a].

[11] In the ocean component of this model, the thermohaline circulation is schematically represented by polar bottom water formation, with the return flow upwelling through the 1-D water column to the surface ocean from where it is returned, through the polar sea, as bottom water to the bottom of the ocean column thereby completing the thermohaline circulation. Climate affects modeled ocean CO_2 uptake through the temperature dependence of CO_2 solubility and carbonate chemistry (i.e., the buffer factor) of the mixed layer. The response of bottom water carbon concentration to changes in the mixed-layer concentration is modeled parametrically by the parameter π_c as described in detail by *Jain et al.* [1995] to account for, e.g., differences in the ventilation of bottom water and the buffer factor of associated surface waters. A marine biosphere source term is included in the deep sea associated with the oxidation of the organic debris exported from the mixed layer where it is produced by photosynthesis [*Volk and Hoffert*, 1985; *Jain et al.*, 1995].

[12] The calibration of the ISAM terrestrial and ocean carbon cycle components to match the range of behavior of results of model intercomparisons of detailed terrestrial and ocean component models is described in sections 2.2.1 and 2.2.2, respectively. The ISAM climate model and parameter ranges are described in section 2.2.3. The range of integrated system response is calculated by running ISAM with the ranges of parameters determined in this way. Results are presented for past carbon cycle in section 4, and for future scenarios in section 5.

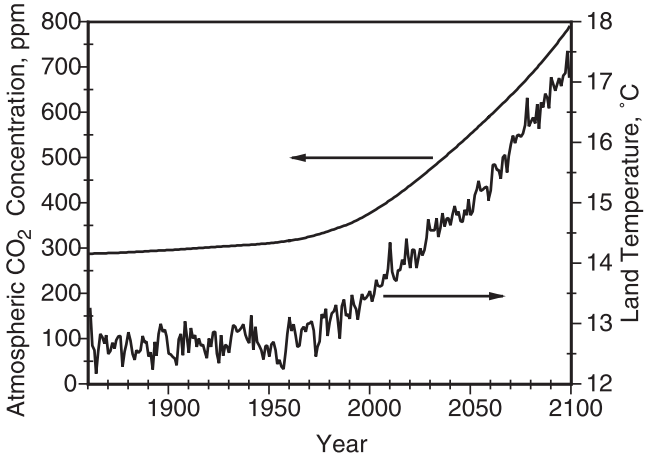

Figure 2. Scenario for atmospheric CO_2 concentration and average land temperature (excluding Antarctica) used in model intercomparisons.

2.2. ISAM Calibrations

2.2.1. Terrestrial Carbon Cycle

[13] The terrestrial (plants, litter, and soils) component of ISAM is calibrated to reproduce the net terrestrial uptake over a decade to century timescale of six Dynamic Global Vegetation Models (DGVMs) that have been intercompared for a common scenario of CO_2 and climate.

[14] The DGVM intercomparison summarized by *Cramer et al.* [2001] report the results of six DGVMs: HYBRID [*Friend et al.*, 1997], IBIS [*Foley et al.*, 1996], LPJ [*Sitch*, 2000], SDGVM [*Woodward et al.*, 1998], TRIFFID [*Huntingford et al.*, 2000], and VECODE [*Brovkin et al.*, 1997]. Each model simulates linked changes in ecosystem function (water, energy, and carbon exchange) and vegetation structure (distribution, physiognomy) in response to a common scenario of changes in CO_2 concentration and climate. The CO_2 concentration scenario, shown in Figure 2, was associated with IPCC emission scenario IS92a [*Leggett et al.*, 1992]: cf. the analysis of IS92a from this study in section 4.1. This same CO_2 scenario was used as input for the coupled atmosphere-ocean general circulation model HadCM2-SUL [*Mitchell et al.*, 1995] to calculate a simulation of the climate response to the IPCC emission scenario IS92a. This climate simulation was the climate scenario used in this intercomparison with some modification [see *Cramer et al.*, 2001]. The annual global land temperature of this modified scenario is shown in Figure 2.

[15] The results of the DGVMs show considerable variability in the terrestrial uptake of carbon in addition to their response to changing CO_2 and climate. Figure 3 shows a 10-year running mean of annual global uptake for the DGVM results corresponding to the common scenario for changing CO_2 and climate. Variations in the 10-year budget of carbon uptake are of similar magnitude to the mean uptake over the past two decades for some models. Year-to-

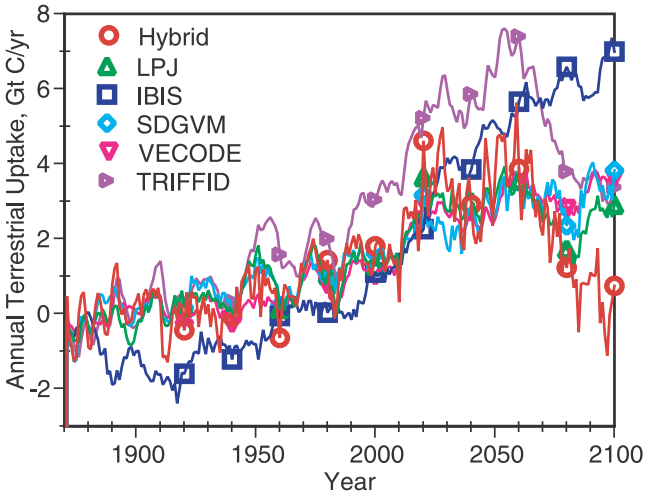

Figure 3. Ten year running mean of annual uptake from six dynamic global vegetation models (DGVMs) in response to a common scenario for atmospheric CO_2 concentration and climate (see Figure 2) [*Cramer et al.*, 2001].

year variations are larger. Over the period from 2000 to 2050, all models show significant carbon uptake in response to the scenario. Beyond 2050, all models, except for the HYBRID model, exhibit continued uptake.

[16] The globally aggregated terrestrial component of ISAM used in this study is driven by changes in atmospheric CO_2, temperature, and land use. Since results from the work of *Cramer et al.* [2001] do not include land use, the absence of land use (preanthropogenic conditions) is specified in ISAM for comparison to DGVM results. Since the future cumulative change in carbon stocks in the terrestrial biosphere is more closely related to change in future atmospheric CO_2 concentration over the next century than annual uptake, ISAM is calibrated to match this feature of the DGVM results shown in Figure 4.

[17] In the first step of the ISAM calibration, the strength of the modeled CO_2 fertilization effect, represented by model parameter β, is adjusted to match DGVM results driven by changes in atmospheric CO_2 concentration with no change in climate. As a "reference" case, the results of ISAM matching the average of the results of the IBIS, LPJ, and SDGVM models corresponds to $\beta = 0.52$. Note that a stronger terrestrial sink would correspond to a larger value of β and a "lower" projection of future CO_2. To define a range of model responses, model parameters corresponding to "low" and "high" projections of CO_2 are estimated. The range of DGVM responses are spanned by ISAM results with $\beta = 0.35$ (high parameterization) to 0.9 (low parameterization): see Figure 4a. Note that the value of β used in ISAM projections for the IPCC SAR was 0.39 [*Jain et al.*, 1996], at the low end of this range; however, the results used in the SAR did not include the feedback of climate on carbon cycle.

[18] In the second step of the ISAM calibration, the strength of the modeled temperature effects on productivity of nonwoody tree parts and the translocation from nonwoody to woody tree parts, represented by model parameters $Q_{10,np}$ and $Q_{10,t}$, are adjusted to match DGVM results driven by changes in both atmospheric CO_2 concentration and climate. The Q_{10} coefficients for temperature sensitivity of respiration and exchange between other soil and plant reservoirs remain unchanged from their values used in prior studies [*Harvey*, 1989a; *Kheshgi et al.*, 1996]. We choose to adjust the Q_{10} coefficients related to NPP because the sensitivity of NPP of DGVMs to increases in temperature differs drastically (even in sign) between DGVMs [*Cramer et al.*, 1999]. We note that the only climate input to ISAM is annual global land temperature, taken as an anomaly from the 1861 to 1900 average land temperature shown in Figure 2. Since the ISAM model is calibrated to match DGVM results, ISAM implicitly includes the effects of the other aspects of the DGVM climate scenario (e.g., regional, seasonal, and diurnal changes in temperature, precipitation, and cloudiness); how good this implicit approximation is

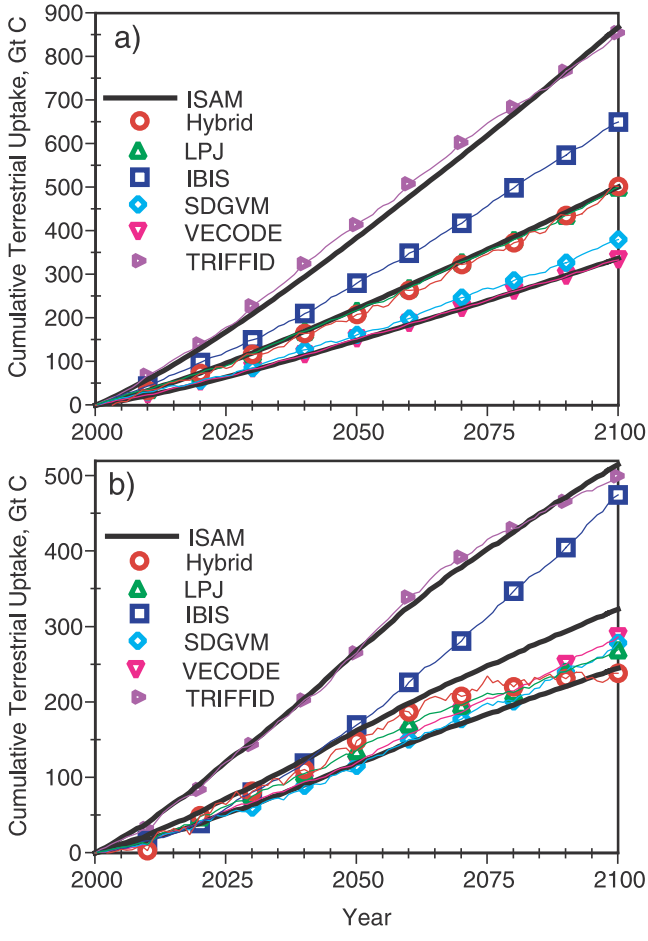

Figure 4. Comparison of modeled accumulation of carbon by plants, soils, and detritus in response to (a) changes in atmospheric CO_2 concentration only and (b) changes in atmospheric CO_2 concentration and climate (see Figure 2). Accumulation counted starting in year 2000. Results of three parameterizations of ISAM (thick black curves) calibrated to match the average (of the LPJ, IBIS, and SDGVM) and range of the six DGVMs.

could be tested by comparing to DGVM results driven by other climate scenarios, however, these are not available. In addition, other potential drivers such as nitrogen deposition and changes in ozone levels are neglected in both the DGVM and ISAM results. These additional effects contribute to the uncertainty in projections and remain to be evaluated.

[19] The reference, low and high ISAM parameterization is estimated to reproduce the terrestrial carbon accumulation response to climate change exhibited by the DGVMs over the time period from 2000 to 2100 (see Figure 4b). For the reference, low, and high parameterizations the Q_{10} coefficient for net productivity of the nonwoody carbon reservoir (see Figure 1) is 1, 0.75, and 1.2, respectively: all are lower than in prior studies [*Harvey*, 1989a; *Kheshgi et al.*, 1996]. For all three parameterizations, the Q_{10} coefficient for translocation from the nonwoody to woody reservoirs is reduced to 1.2 from that in prior studies to avoid an excessive buildup in the nonwoody reservoir. While productivity in these parameterizations of ISAM all increase with increasing temperature, productivity does not increase as much as does respiration. The net result is less terrestrial carbon accumulation compared to the results (Figure 4a) without climate change. Note that the low parameterization has both a stronger modeled CO_2 fertilization effect and a weaker temperature productivity sensitivity than the reference case. The high parameterization has the opposite. The effect of increasing temperature, therefore decreases the width of the range of modeled terrestrial carbon accumulation from that without climate change.

2.2.2. Ocean Carbon Cycle

[20] The ocean component of ISAM is calibrated to reproduce the net ocean uptake over a decade to century timescale of 10 detailed ocean carbon cycle models that have been intercompared for the common scenario of CO_2 given in Figure 2.

[21] The ocean model intercomparison organized under the Ocean Model Intercomparison Project (OCMIP) [*Orr and Dutay*, 1999] provided the results [*Prentice et al.*, 2001] of 10 detailed ocean carbon cycle models labeled with the acronyms: (1) Alfred Wegener Institute (AWI) for Polar and Marine Research, Bremerhaven, Germany; (2) CSIRO, Hobart, Australia; (3) IGCR (IGCR/CCSR), Tokyo, Japan; (4) Institute Pierre Simon LaPlace (IPSL), Paris, France; (5) LLNL, Livermore, California, USA; (6) Max Planck Institut fuer Meteorologie (MPIM), Hamburg, Germany; (7) National Center for Atmospheric Research (NCAR), Boulder, Colorado, USA; (8) Physics Institute (PIUB), University of Bern, Switzerland; (9) Princeton University (PRINCE, AOS, OTL)/GFDL, Princeton, New Jersey, USA; and (10) Southampton Oceanography Centre (SOC)/SUDO/Hadley Center, UK Met. Office, England.

[22] The ocean CO_2 uptake response of the OCMIP models to changing atmospheric CO_2 concentration is shown in Figure 5. All of the responses show an increasing uptake of carbon. Variability in annual uptake is small in comparison to the magnitude of uptake, unlike the results of DGVMs. Accumulation of carbon in the oceans from 2000 to 2100 (Figure 5b) is of comparable magnitude to that of the modeled terrestrial biosphere (Figure 4).

[23] The response of the globally aggregated ocean component of ISAM, used in this study, to atmospheric CO_2 depends on ocean transport parameters: effective vertical diffusivity, upwelling velocity, and the change in bottom water concentration relative to the change in mixed layer concentration is modeled parametrically by the parameter π_c. The latter parameter is poorly constrained by ocean tracers and has a large effect on the ocean carbon budget over a decade to century timescale [*Kheshgi et al.*, 1999]. ISAM is calibrated to match the average and range of all 10 OCMIP responses by adjustment of parameter π_c leaving remaining ocean parameters at the values used in prior studies [*Jain et al.*, 1995; *Kheshgi et al.*, 1999]. The average response of the OCMIP models is matched using $\pi_c = 0.475$, and the range is spanned with $\pi_c = 0.807$ (low parameterization) to $\pi_c = 0.072$ (high parameterization) compared with $\pi_c = 0.5$ used in prior studies [*Jain et al.*, 1995; *Schimel et al.*, 1995, 1996]. Comparison between the annual and cumulative uptake of ISAM calibrated in this way is compared to that of the 10 OCMIP models in Figure 5.

[24] As noted by *Prentice et al.* [2001] and references therein, the effects of temperature on total dissolved carbon solubility dominate the modeled climate's effect on ocean uptake for scenarios such as this one prior to 2050. After that time, changes in ocean stratification begin to slow modeled ocean uptake further in coupled ocean carbon cycle/climate simulations. The comparison to OCMIP results presented here did not include effects of changing climate. ISAM does include effects of ocean surface temperature on total dissolved carbon solubility: we expect that the ISAM aggregated model for this effect will accurately reproduce this effect as seen in detailed models [cf. *Kheshgi and White*, 1996]. ISAM does not, however, include effects of climate on ocean stratification.

2.2.3. Climate/Carbon System

[25] In ISAM, a reduced form energy balance climate model of the type used in the 1990 IPCC assessment [*Hoffert et al.*, 1980; *Bretherton et al.*, 1990] is used to calculate global and annual mean near-surface temperature. In this energy balance model, radiative forcing of climate is balanced by accumulation of heat in the oceans and enhanced outgoing (infrared) radiation due to increased global temperature.

[26] Radiative forcing of climate is calculated from the same relations between greenhouse gas concentrations and aerosols as was used in the IPCC TAR [*Ramaswamy et al.*, 2001]. Notably, the radiative forcing for a doubling of CO_2 concentration is $\Delta F_{2x} = 3.7$ W m^{-2} [*Ramaswamy et al.*, 2001], a 15% lower radiative forcing compared with the value of 4.37 W m^{-2} used in previous assessments [*Harvey et al.*, 1997].

[27] The primary factor relating radiative forcing change to global temperature change in the ISAM model is the equilibrium climate sensitivity for a doubling of CO_2 concentration, ΔT_{2x}. Equilibrium climate sensitivity is one factor used to account for the uncertainty in future global climate projections even though a full characterization of uncertainty of climate projections is not well characterized [e.g., *Morgan and Keith*, 1995]. We use a reference value of climate sensitivity of 2.5°C for a radiative forcing increase

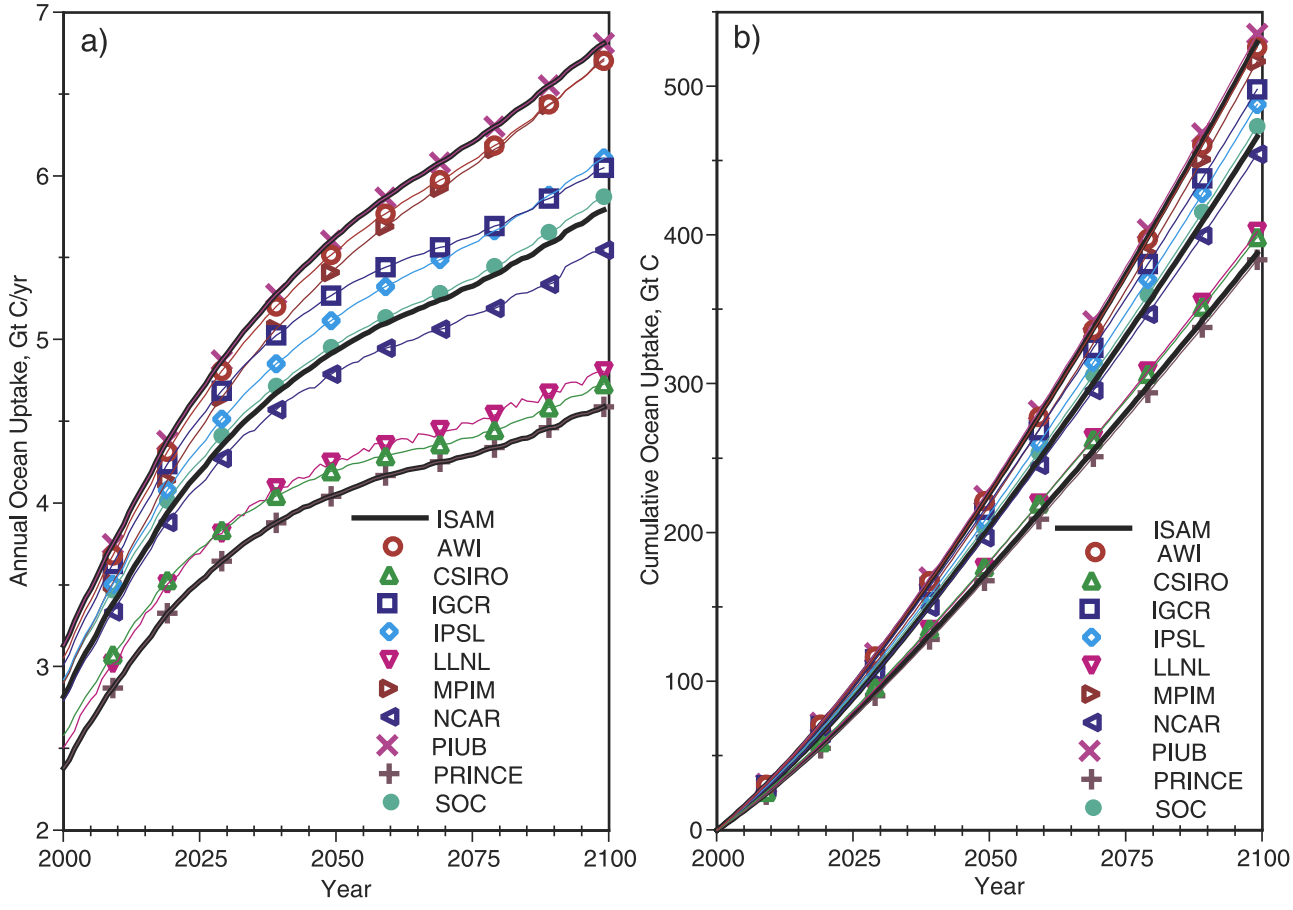

Figure 5. Comparison of modeled (a) annual uptake and (b) accumulation of carbon in the oceans in response to changes in atmospheric CO_2 concentration following the CO_2 scenario shown in Figure 2. Accumulation counted starting in year 2000. Results of three parameterizations of ISAM (thick black curves) calibrated to match the average and range of the 10 coupled ocean/atmosphere models.

produced by doubling of CO_2, and test the sensitivity to this parameter over the range of climate sensitivity from 1.5° to 4.5°C, the range still considered to be appropriate by the IPCC [*Cubasch et al.*, 2001]. Since higher temperature is associated with less uptake of CO_2 by the ocean and biosphere in the model intercomparisons, as discussed above, we associate a climate sensitivity of 4.5°C with our high CO_2 parameterization of ISAM and 1.5°C with our low parameterization.

[28] In ISAM, ocean heat transport follows the same transport scheme and parameters as does transport of dissolved inorganic carbon. Therefore for the reference and range of projections calculated in the following sections, the ocean parameters found to fit the ocean carbon cycle results (discussed in section 2.2.2) are used as well for ocean heat transport.

[29] Global temperature change projected by the model is used as an index of climate change, as is land temperature change in section 2.2.2. All coupled ocean/atmosphere general circulation models appear to exhibit greater warming over land than over the oceans when forced with increasing greenhouse gas concentrations [*Cubasch et al.*, 2001]. To approximate this effect, the land temperature anomaly (from the preanthropogenic model equilibrium) is taken to be 25% larger than the global temperature change calculated by the ISAM energy balance model. This land temperature change is used as input to the terrestrial carbon cycle component of ISAM for both projections of future climate change using ISAM projections of global temperature anomaly, as well as past reconstructions using observation-based estimates of global temperature anomaly.

[30] There are other factors influencing climate (solar fluctuations, volcanoes, ocean current variations) that result in climate variability that is not represented in ISAM projections. In addition, there is considerable uncertainty in the radiative forcing of climate from, e.g., aerosols [*Schwartz and Andreae*, 1996], that are not considered in this study. Furthermore, this study uses global mean annual temperature anomaly as a proxy for climate change that affects global carbon cycle. Uncertainty in, e.g., regional patterns of temperature and precipitation will add to the uncertainty in carbon storage in plants also not accounted for in this study. Ranges of reported results are, therefore

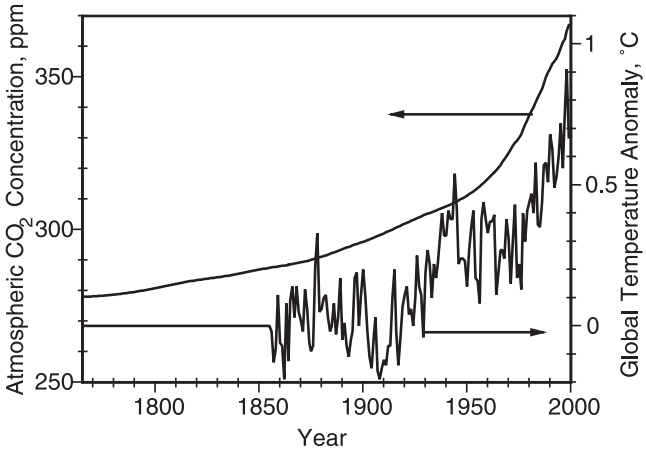

Figure 6. Observation-based estimates of global temperature anomaly and atmospheric CO_2 specified as inputs for ISAM over the period from 1765 to 1999 for reconstruction of past carbon cycle and computation of initial conditions for future projections.

intended to form a lower bound on the plausible range of future carbon cycle response.

3. Reconstruction of Past Carbon Cycle

[31] The ISAM model is used to reconstruct the past globally aggregated response of carbon cycle to observed changes in atmospheric CO_2, temperature, and estimated fossil fuel emissions for the three different model parameterizations. ISAM reconstructions start from a steady state model solution with temperature anomaly equal to 0 and atmospheric CO_2 of 278 ppm. The model solutions span from 1765 through 1999.

[32] Figure 6 shows the atmospheric CO_2 and temperature inputs for ISAM over the period from 1765 through 1999. Estimates of atmospheric CO_2 concentration from ice cores and direct measurements given by *Enting et al.* [1994] are specified from 1765 through 1972. The average of annual concentrations from the Mauna Loa (Hawaii) and South Pole Observatories [*Keeling and Whorf*, 2000] is specified for the period from 1973 through 1999. The annual globally aggregated near-surface temperature estimated by *Jones et al.* [2000] is specified from 1856 through 1999 as an anomaly from its average from 1856 through 1875 (for prior times, 1765 through 1855, it is set to zero). Estimates of global annual emissions from fossil fuel burning and cement production made by *Marland et al.* [2000] are specified from 1765 through 1997. Emissions for 1998 and 1999 are estimated by applying emission factors [*IPCC*, 1997] to energy consumption statistics [*British Petroleum Company*, 2000] to calculate emissions over the period from 1997 through 1999; this emission estimate is then scaled to match the *Marland et al.*'s [2000] estimates for emissions from fossil fuel burning and cement production in 1997. The resulting emission estimate for 1998 and 1999, therefore implicitly includes emissions from cement production.

[33] The modeled uptake of CO_2 by the oceans is calculated in response to the specified changes in atmospheric CO_2 and temperature. However, to calculate the net terrestrial (i.e., from plants and soils) source or sink of CO_2 from the terrestrial carbon cycle model requires the additional specification of a history of land use emissions, and estimates of past land use emissions remain very uncertain. To balance the carbon budget, emissions of fossil carbon must equal accumulation of carbon in the atmosphere, ocean, and terrestrial reservoirs. This constraint provides an alternative means to deduce the net terrestrial source of carbon. The land use emission is then deduced to be that required for the model to match this net terrestrial source. The difference between the net terrestrial source and the deduced land use emission is therefore the modeled terrestrial response to changes in atmospheric CO_2 and temperature. The terrestrial response, however, does depend on the history of land use in ISAM, and so a sequential iterative method is used to converge on this match [*Kheshgi et al.*, 1996]. Land use emissions deduced in this way can be compared to independent emission estimates as one test for model consistency.

[34] Model-based reconstruction of carbon budgets over different time periods for the three model parameterizations are given in Table 1. Since fossil CO_2 emissions and atmospheric CO_2 concentration are model inputs independent of model parameterization, the budget quantities for these are common for the three parameterizations.

[35] Modeled ocean uptake is driven by changes in CO_2 and temperature. Temperature rise is particularly strong in *Jones et al.*'s [2000] temperature record over the past two decades (Figure 6). Over periods of rising temperature,

Table 1. Model-Based Reconstructions of Past Carbon Budgets

	Budget Period											
	1980–1989			1990–1999			1850–1989			1765–1999		
Observation-Based Quantities, Gt C												
(a) Fossil CO_2 emissions	54.5			63.3			212.0			276.5		
(b) Atmospheric CO_2 accumulation	33.3			32.9			137.1			189.0		
Model-Based Quantities, Gt C												
Model parameterization ⇒	Ref	Low	High	Ref	Low	High	Ref	Low	High	Ref	Low	High
(c) Ocean sink	16.5	18.2	14.4	18.6	20.6	16.0	93.7	104.6	80.1	125.2	139.2	107.8
(d) Net terrestrial sink (=a-b-c)	4.6	2.9	6.8	11.8	9.7	14.4	−18.9	−29.8	−5.2	−37.7	−51.6	−20.3
(e) Terrestrial sink in response to climate and CO_2 change	13.3	22.8	9.2	15.0	25.0	10.8	77.5	133.2	54.1	103.5	178.2	71.9
(f) Land use source (=e-d)	8.7	19.9	2.4	3.2	15.2	−3.6	96.3	163.0	81.8	141.2	229.9	92.2

modeled ocean uptake is lower than if temperature did not change. This causes modeled ocean uptake over the 1980s and 1990s to be lower by about 3 Gt C (0.3 Gt C/yr) over each decade (Table 1) than in the ocean model intercomparison without climate change.

[36] In early IPCC assessments of carbon budgets [*Schimel et al.*, 1995], the ocean sink of carbon in the 1980s was estimated to be 20 ± 8 Gt C (90% confidence interval) which is based primarily on ocean carbon cycle models calibrated with bomb-radiocarbon constraints; extending these models to the 1990s gave an estimate of 23 ± 8 Gt C [*Bolin et al.*, 2000]. Inclusion of both ^{13}C and ^{14}C constraints, along with modeled temperature change, led to a slightly lower estimate of 17 ± 7 Gt C (90% confidence interval) for the 1980s [*Kheshgi et al.*, 1999]. O_2/N_2 data available for the 1990s has led to a nearly model independent estimate of 17 ± 8 Gt C (90% confidence interval) for the 1990s [*Prentice et al.*, 2001], although this estimate is sensitive to various corrections for temperature change [*Le Quéré et al.*, 2001]. In addition, the net ocean uptake of CO_2 due to the entire anthropogenic perturbation of carbon cycle has been estimated indirectly using oceanic observations [*Gruber et al.*, 1996]; for the period up until 1990, a global estimate of 107 ± 27 Gt C [one standard error, see *Prentice et al.*, 2001] has been made which compares well with the reference case value of 106.6 Gt C (Table 1). The ISAM range of ocean uptakes for these decades listed in Table 1 are within all of these uncertainty ranges and spans a narrower range.

[37] In IPCC assessments of the past carbon budget, the net terrestrial sink was deduced from the budget given an estimate of fossil fuel emissions, atmospheric emissions, and ocean uptake [*Watson et al.*, 1990; *Schimel et al.*, 1995, 1996; *Bolin et al.*, 2000; *Prentice et al.*, 2001]. A residual terrestrial sink was deduced from the budget using estimates of land use emissions. This sink was then compared to estimates of sinks due to different factors: CO_2 and nitrogen fertilization and climate change [*Schimel et al.*, 1995].

[38] In this model reconstruction of the past carbon budget, ranges of net terrestrial uptake are calculated from the budgets in Table 1 and therefore depend on ranges of ocean model uptake. Land use emissions are then deduced from the difference between net terrestrial uptake and the modeled terrestrial sink [an example of the time history of land use emissions deduced in this way is shown in Figure 3 of *Kheshgi et al.*, 1996]. Unlike the IPCC budgets, however, ranges of land use emissions listed in Table 1 are deduced, based on ranges of terrestrial model responses (to temperature and CO_2). Land use emissions deduced from the modeled carbon budget in this way can be compared to land use emission estimates based on surveys of land use change, and forest and soil carbon data. Survey-based estimates of land use emissions are, for example, 17 ± 8 Gt C [*Bolin et al.*, 2000; *Houghton*, 2000] for the decade of the 1980s, and 16 ± 8 Gt C [*Bolin et al.*, 2000] for the 1990s. The ranges of budget-deduced land use emissions in Table 1 (row f), however, extend to much lower values, especially in the 1990s. Estimates of land use emissions may well form a constraint on this range of model results. There could, however, be considerable decadal variability in terrestrial carbon uptake, as is evident in the responses of the DGVMs in Figure 3. Variability must be accounted for land use emission estimates that are used as a constraint on the range of terrestrial model response; this was neglected in past IPCC assessments [*Schimel et al.*, 1995, 1996]. Observed terrestrial carbon uptake over a single decade will be of limited use to calibrate terrestrial carbon cycle models until variability in terrestrial uptake is understood. Consideration of longer budget periods (cf. Table 1) may mute this effect of variability of terrestrial CO_2 uptake. Changes in land uses have led to an estimated net emission of CO_2 of 121 Gt C from 1850 to 1990 [*Houghton*, 1999, 2000], as well as an estimated 60 Gt C prior to 1850 [*DeFries et al.*, 1999]. These estimates are well within the range of model budget deduced land use emissions in Table 1.

4. Projections of Future Carbon Cycle

4.1. IS92a Benchmark Scenario

[39] Model-based estimates of CO_2 concentration, the global carbon budget, and climate effects are extended into the future by specification of scenarios of CO_2 emissions from fossil fuels and land use, as well as the emission of other greenhouse gases (CH_4, N_2O, CFCs, and HCFCs), aerosols, and aerosol precursors. In this section, the IPCC emission scenario IS92a [*Leggett et al.*, 1992] is used as a benchmark to compare model studies over the time period from 2000 to 2100. The fossil CO_2 emissions for this scenario are shown in Figure 7a.

[40] Extending from the past ISAM reconstructions (section 3) to the year 2100, projections are made with the three parameterizations of ISAM including the range of climate sensitivities discussed in section 2.2.3. The carbon budgets for these projections from 2000 through 2099 is summarized in Table 2, CO_2 concentrations are given in Figure 7b, and projected global temperature anomalies in Figure 7c. A single estimate of radiative forcing (as a function of time) from other greenhouse gases and aerosols is input over this time period consistent with that given in the IPCC TAR [*Ramaswamy et al.*, 2001], therefore the sensitivity to uncertainties in these contributors to radiative forcing are not included.

[41] ISAM projections for the IS92a scenario in 2100 for the reference (low, high) parameterization of CO_2 concentration are 723 ppm (640–804 ppm). As is evident in the carbon budget in Table 2, the range in accumulation of plant and soil carbon stocks is the primary source of the width of range in atmospheric CO_2 concentration projections. Projected global temperature anomaly (i.e., the change from the 1765 ISAM equilibrium) in 2100 is 2.9°C (1.7°–5.6°C) as shown in Figure 7c. The difference between the projected global temperature anomaly in 2100 and the observation-based anomaly in 1990, taken to be 0.68°C, is therefore 2.2°C (1.0°–4.9°C). The range in climate sensitivity and CO_2 concentration both contribute to the range in projected temperature in 2100 with climate sensitivity being the primary factor.

[42] For the IS92a benchmark scenario, the IPCC SRRF [*Schimel et al.*, 1995] presented the results of an intercomparison of 18 global carbon cycle models [*Enting et al.*,

1994]. The terrestrial carbon cycle components of these models did not include the range of processes (e.g., the effects of disturbance) or the geographical detail of the models with results summarized in Figures 3 and 4. Furthermore, in the intercomparison, the terrestrial components were calibrated to match the central estimate of the global carbon budget for the 1980s with a CO_2 emission from changing land use over the 1980s, referred to as Dn80s in the IPCC SAR [*Schimel et al.*, 1996; *Wigley et al.*, 1997], of 16 Gt C (compare with Table 1). This intercomparison yielded CO_2 concentration projections in 2100 ranging from 668 to 734 ppm, a range of width of 66 ppm compared to a range of 164 ppm for the ISAM results presented here and in the IPCC TAR. Illustrated results in the IPCC SRRF were those of the Bern model [*Siegenthaler and Joos*, 1992] that gave 688 ppm in 2100.

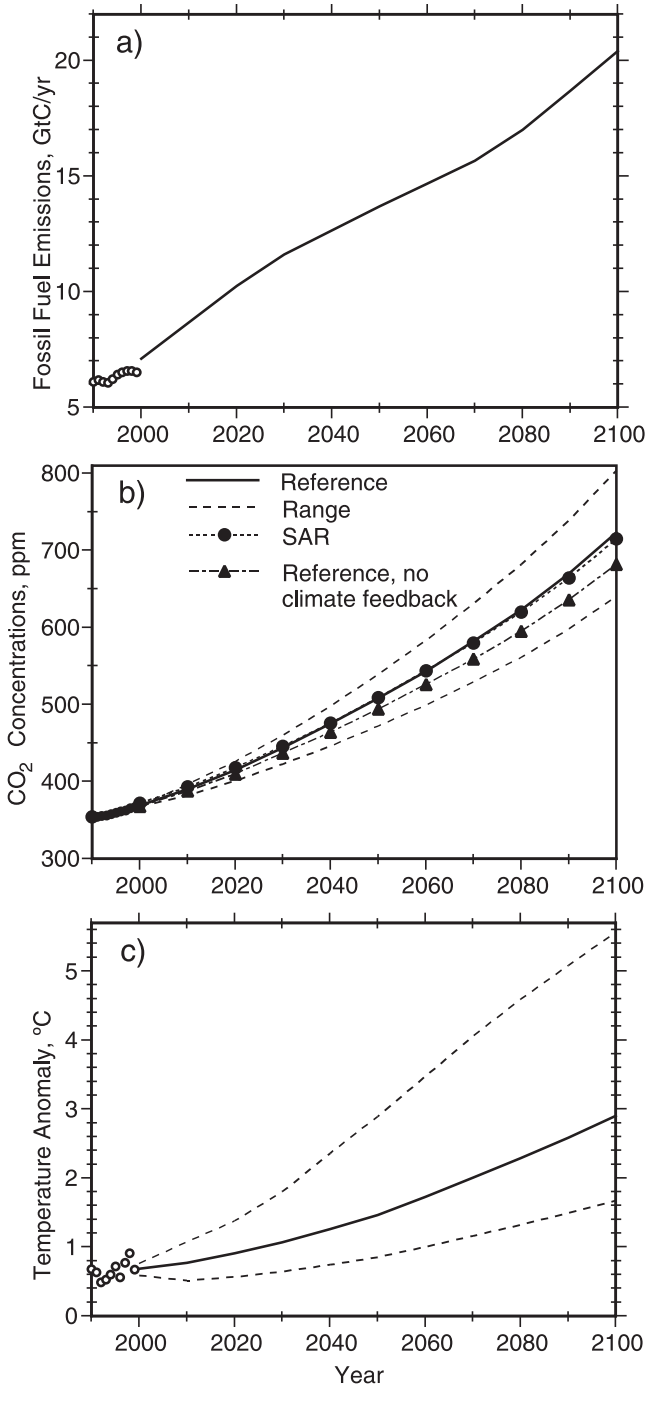

Figure 7. (opposite) Projections of CO_2 concentration and global average near-surface temperature driven by the benchmark emission scenario IS92a [*Leggett et al.*, 1992]. (a) This future nonintervention emission scenario for CO_2 emissions from fossil fuels and cement production is shown. Specifying this scenario, (b) the solid curves show the ISAM projections (using the reference parameterization) of CO_2 concentrations, and (c) global temperatures. Temperature is given as an anomaly from mid-1800s (see section 4.3 and Figure 6). The highest and lowest projections (high and low parameterizations of ISAM) are shown by the dashed curves. Projected CO_2 concentrations are also shown by the labeled curves when the climate/carbon cycle interaction is not included (for reference ISAM parameters) and as reported in the IPCC SAR [*Schimel et al.*, 1996]. Observation-based estimates are shown by the circles prior to 2000.

[43] The IPCC SAR [*Schimel et al.*, 1996] revised the projections given in the IPCC SRRF, in response to a revised 1980s carbon budget. The IPCC SAR 1980s budget had a CO_2 emission from changing land use over the 1980s of 11 Gt C. When the strength of the CO_2 fertilization effect in the Bern model was weakened to match this 1980s budget, the CO_2 concentration projection in 2100 increased to 712 ppm. The parameterization of the ISAM model used for the IPCC SAR (with climate effects on carbon cycle neglected) gave a similar CO_2 concentration projection in 2100 of 715 ppm (see Figure 7b for SAR result). *Wigley et al.* [1997] found CO_2 concentration projections in 2100 ranged from 667 to 766 ppm, a range of width 99 ppm, when uncertainty in land use emission estimates were taken into account (Dn80s taken to range from 18 to 4 Gt C) in calibrations of the CO_2 fertilization effect. This range is narrower than presented here even though this study starts its projections in 2000, rather than in 1990 as in the SAR. Note that the reference parameterization of ISAM has a stronger CO_2 fertilization effect than in the SAR which is compensated by climate feedbacks not included in SAR projections resulting in a CO_2 projection nearly identical to the SAR (see Figure 7b). The range of projected temperature increase between 1990 and 2100 quoted from the IPCC SAR based on the range of IS92 scenarios is 1.0°–3.5°C, narrower than the range of temperatures presented here for only one (near the center) emission scenario, IS92a.

[44] In the IPCC TAR, CO_2 concentration projection of both the ISAM model (with parameters described here and projections as included here) and *Joos et al.*'s [2001] model were illustrated. The projections based on *Joos et al.*'s [2001] model specified ranges of model input parameters that were thought to be the outer limits of possible parameter ranges. If, indeed, these are the outer limits, and if ranges of all relevant uncertain parameters are included, then that range would represent an upper bound on the range of projected CO_2 concentration (of course under the

Table 2. Carbon Budgets for the 21st Century for IPCC Emission Scenarios

	Change in Carbon Stocks from 2000 to 2099, Gt C[a]										
			Plants and Soils[b]			Oceans			Atmosphere		
Model parameterization⇒	Fossil Fuels[a]	Land Use	Ref	Low	High	Ref	Low	High	Ref	Low	High
IPCC scenario											
IS92a	−1360.4	−68.2	236.5	401.6	130.7	379.6	389.2	317.3	744.2	569.5	912.4
A1B	−1363.6	−50.3	242.2	412.4	150.3	385.1	397.8	324.2	736.3	553.5	889.1
A1T	−968.5	−19.4	200.1	330.6	126.2	312.9	321.2	261.0	455.5	316.7	581.3
A1FI	−2046.2	−50.9	313.8	537.5	199.2	469.6	495.6	392.4	1262.8	1013.2	1454.6
A2	−1695.9	−77.5	253.4	445.9	153.6	422.8	441.0	356.1	1019.7	809.1	1186.2
B1	−919.4	16.8	236.0	355.5	167.5	297.8	302.5	252.0	385.6	261.3	499.9
B2	−1086.0	7.4	238.6	371.7	165.3	314.5	322.9	264.5	532.9	391.5	656.3

[a]Budget period extends from the start of 2000 to the end of 2099. This leads to a slight discrepancy with the cumulative emissions reported in the IPCC Special Report on Emission Scenarios that apparently accumulates emissions from midyear to midyear, provided the reported emissions are per annum as is consistent with the initial (1990) emissions data. Negative changes in fossil fuel and land use carbon stocks equates to positive cumulative fossil fuel and land use emissions.

[b]The change in plant and soil carbon stocks includes that due to land use change, an equivalent definition to row e in Table 1.

specifications of the scenario: emissions and certain radiative forcing from radiative forcing agents other than CO_2). Indeed, the IS92a CO_2 concentration projections of *Joos et al.*'s [2001] model are wider, 703 ppm (632–902 ppm) by 2100, than the ISAM projections presented here and in the IPCC TAR.

[45] Other studies give varied results. In the DGVM intercomparison described in section 2.2, nominally a simulation of the IS92a scenario based on results from the Hadley Center, the specified CO_2 concentration in 2100 was 790 ppm [*Cramer et al.*, 2001], near the high end of the ISAM range. Furthermore, *Cox et al.* [2000] find that with a global carbon cycle model including a variant of the TRIFFID model when combined with another Hadley Center climate model (HADCM-3) and climate drivers (no aerosols), but still nominally for the IS92a scenario, led to considerably less accumulation of carbon in soils than would be represented by the range of ISAM results. Over the period from 2000 through 2099, *Cox et al.* [2000] reported plants and soils were a source of CO_2 rather than a sink as given in Table 2, and led to a CO_2 concentration projection in 2100 of 980 ppm, above both the ranges produced with ISAM and with *Joos et al.*'s [2001] model.

4.2. SRES Scenarios

[46] A set of 40 emission scenarios was reported in the IPCC Special Report on Emission Scenarios (SRES) [*Nakicenovic et al.*, 2000] and was intended to improve on the earlier set of six scenarios that include the IS92a benchmark considered in section 4.1. These are scenarios intended to exclude emission controls to limit climate change, sometimes referred to as "nonintervention" scenarios. Future emissions of greenhouse gases and aerosols are determined by driving forces such as population, socio-economic development, and technological change, and hence are highly uncertain. The 40 SRES scenarios consist of four scenario groups (labeled A1, B1, A2, and B2), based on narrative storylines, which span a wide range of these driving forces. They encompass four combinations of demographic change, and social and economic development. Scenario group A1 is further split into three scenario groups, A1B, A1FI, and A1T that explicitly explore alternative directions for energy technology in the energy system. In this study, we consider only the six scenarios, labeled marker or illustrative scenarios in the IPCC SRES [*Nakicenovic et al.*, 2000], that are illustrative of the six groups.

[47] Fossil carbon dioxide emissions for these six SRES scenarios are summarized in Table 2 and Figure 8a. The two scenarios with the lowest CO_2 emissions are the B1 scenario characterized by a storyline emphasizing environmental and societal sustainability, and the A1T scenario characterized by a storyline emphasizing rapid economic growth along with rapid development and implementation of nonfossil energy sources. The scenario with most rapidly increasing emissions, A1FI, on the other hand, is characterized by a storyline emphasizing rapid economic growth and carbon-intensive energy supply systems, whereas the A1B storyline has a "balance" between nonfossil and fossil energy systems. The A2 storyline assumes slow regional economic growth. The B2 storyline has intermediate levels of economic growth with less rapid technological development than A1 or B1.

[48] The SRES scenarios also include emissions of CO_2 from land use, emissions of other greenhouse gases, as well as aerosols, and aerosol and ozone precursors. It should be noted that the cumulative land use emissions over the next century for these scenarios (Table 2) are but a few percent of total stocks of carbon in plants and soils. The modeled change in global NPP and productive land cover is therefore a similarly small fraction of the total. To model the effect on the climate/carbon cycle system, we adopt the contributions of non-CO_2 greenhouse gases and aerosols to the total radiative forcing of climate listed in the IPCC TAR [*Ramaswamy et al.*, 2001]. It is important to note that these contributions do not include an appreciable net contribution from nonsulfate aerosols, any radiative forcing (e.g., albedo and humidity effects) from land cover change, nor account for any natural variations in radiative forcing (e.g., future volcanoes and solar variations could contribute to future radiative forcing and, if not predictable, further contribute the range of uncertainty in forecasts of future climate). Furthermore, the uncertainty in the radiative forcing effect of aerosols, which is not well characterized [*Ramaswamy et al.*, 2001], remains a primary contributor to the uncertainty in radiative forcing [*Schwartz and Andreae*, 1996] that is

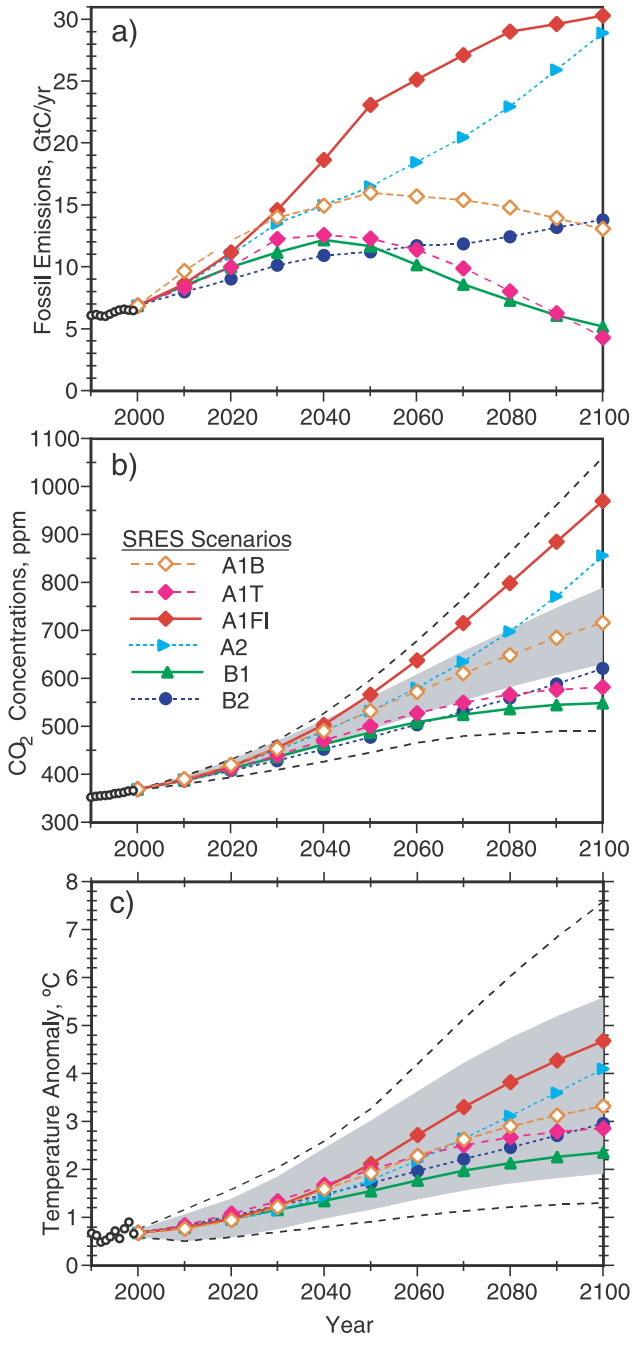

Figure 8. Projections of CO_2 concentration and global average near-surface temperature driven by the IPCC SRES [*Nakicenovic et al.*, 2000] emission scenarios. (a) The six illustrative scenarios of CO_2 emissions from fossil fuels and cement production are shown. Projections of (b) CO_2 concentrations and (c) global temperatures for the six scenarios are shown by the plotted symbols for the reference parameterization of ISAM. Temperature is given as an anomaly from mid-1800s (see section 4.3 and Figure 6). The highest and lowest projections (high and low parameterizations of ISAM) are shown by the shaded area for only scenario A1B and for all six scenarios by the dashed curves. Observation-based estimates are shown by the circles prior to 2000.

not included. By neglecting these uncertainties, as is done here and in the climate change projections of the IPCC TAR [*Cubasch et al.*, 2001], we omit important contributors to the uncertainty in climate projections to be considered when drawing implications of these climate change projections.

[49] A heavily communicated feature of the *IPCC* TAR [2001b] was the higher range (1.4°–5.8°C) of projected global temperature increase from 1990 to 2100 than was reported (1.0°–3.5°C) in the IPCC SAR [*Kattenburg et al.*, 1996]. The cause of the higher projections was the lower emission rates of SO_2, a precursor to sulfate aerosols modeled to be a global cooling agent, specified in the SRES scenarios compared to the scenarios [*Leggett et al.*, 1992] used to make the IPCC SAR projections. The reason for reducing the SO_2 emission rate in the SRES scenarios was the expectation that SO_2 emission controls would be stronger than assumed in the previous set of scenarios [*Nakicenovic et al.*, 2000]. While the SRES scenarios were not intended to include emission reductions for the purpose of climate change mitigation, they were intended to include reductions to control pollutants. But, while SO_2 emissions were lowered in SRES, tropospheric ozone precursor emissions were not; since tropospheric ozone is a global warming agent, the seemingly inconsistent reduction of the cooling agent SO_2 without the control of tropospheric ozone results in a higher range of temperature projections than if tropospheric ozone were also controlled [*Wigley and Raper*, 2001]. This led the *IPCC* [2001a] to conclude that a key uncertainty in future projections is "Inadequate emission scenarios for ozone and aerosol precursors." In addition, the *IPCC* [2001a] concluded that another key uncertainty in future projections is "Factors in modeling of carbon cycle including the effects of climate feedbacks"; we begin to address this factor next.

[50] The projected range of CO_2 response to the six SRES scenarios is made using the alternate, reference (low and high CO_2), parameterizations of the ISAM model in the same way as with the IS92a scenario (section 4.1). The CO_2 response is calculated starting from the initial condition in 1999. Observation-based estimates of fossil emissions through 1999 are used to calculate the initial condition, and beginning in 2000 SRES emissions are specified.

[51] Projected CO_2 concentrations are presented in Figure 8b and carbon budgets in Table 2. The alternative CO_2 concentration projections for the different model parameterizations of all six scenarios overlap to some extent up until 2050. Scenario A1FI results in the highest projected CO_2 concentration in 2100 of 970 ppm (851–1062 ppm), followed by A2, A1, B2, A1T, and B1. The lowest, scenario B1, results in a projected CO_2 concentration of 549 ppm (490–603 ppm) in 2100. The range of projections in 2100 for any one scenario is, therefore 27–50% as wide as the range of reference projections for the six different scenarios. The range of projected CO_2 concentrations for the different ISAM parameterizations is primarily due to the modeled range of the change in carbon stocks in plants and soils (Table 2). This range of reference projections, 549–970 ppm in 2100, is slightly higher than the range of reference projections (made with the Bern model) of the IS92 scenarios given in the SAR of 488–944 ppm [cf. *Wigley*, 1999].

Tabulated values of projected CO_2 concentrations and the related radiative forcing estimates are listed in Appendix II of the IPCC TAR [*IPCC*, 2001b].

[52] Projected global mean temperature anomalies are presented in Figure 8c. Scenario A1FI results in the highest projected global mean temperature anomaly in 2100 of 4.7°C (2.8°–7.5°C), followed by A2, A1, B2, A1T, and B1. The lowest, scenario B1, results in a temperature anomaly of 2.4°C (1.3°–4.1°C). The difference between the projected global temperature anomaly in 2100 and the observation-based anomaly in 1990 (0.68°C) is, therefore 4.0°C (2.1°–6.8°C) for A1FI and 1.7°C (0.6°–3.4°C) for B1: an overall range for the six SRES scenarios of 0.6°–6.8°C.

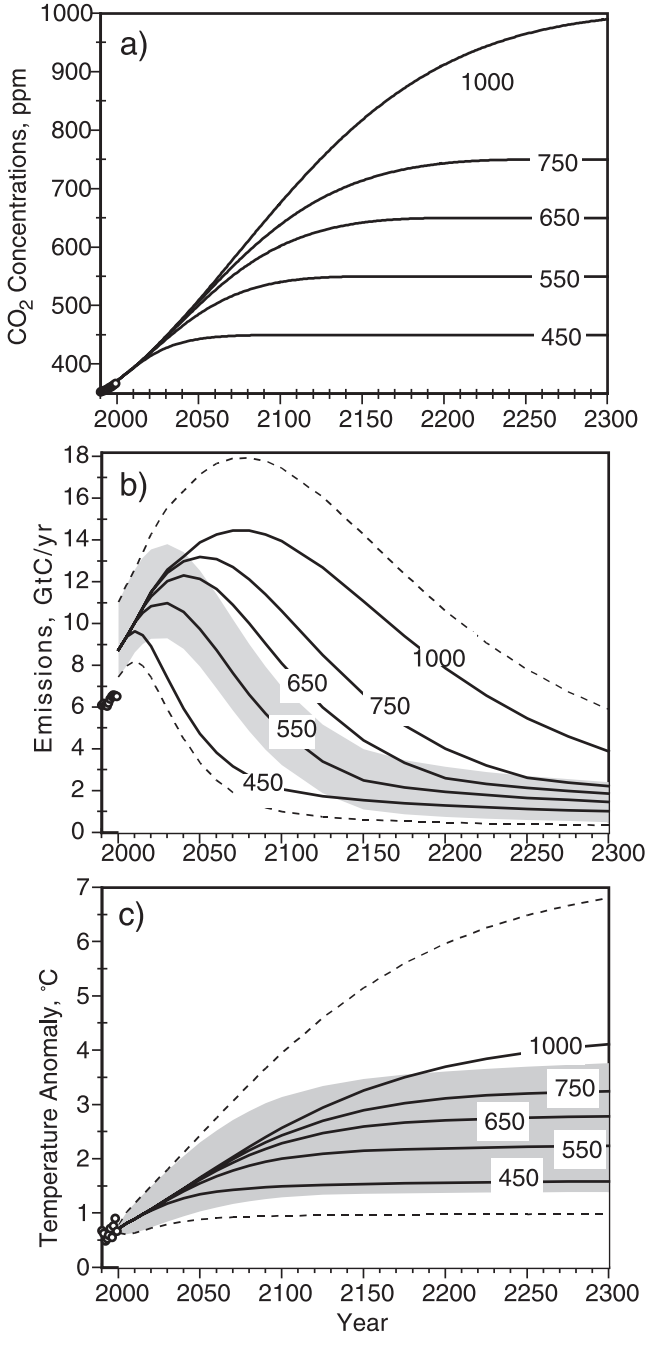

[53] The range of projected temperature increase from 1990 to 2100 in this analysis (0.6°–6.8°C) is wider than the range (1.4°–5.8°C) highlighted in the IPCC TAR [*Cubasch et al.*, 2001]. Furthermore, the IPCC TAR based its range on the full set of SRES scenarios which are projected [*Cubasch et al.*, 2001] to have a slightly wider range of temperature increase than the six marker/illustrative scenarios considered in this analysis. There are several reasons for the wider range of temperature projections in this study:

[54] (1) A wider range of CO_2 concentration projections is found in this study for the six SRES scenarios than was used in the IPCC TAR for the 35 SRES scenarios analyzed [*Wigley and Raper*, 2001]. The wider CO_2 projection range in this study is due to the range of modeled carbon cycle response to a given emission scenario, a contributor to uncertainty not included in the IPCC TAR temperature projections [*Cubasch et al.*, 2001].

[55] (2) A wider range of climate sensitivity, ΔT_{2x} = 1.5° − 4.5°C, is prescribed in this study than in the IPCC TAR where ΔT_{2x} = 1.7° − 4.2°C [*Cubasch et al.*, 2001].

[56] (3) Finally, in this study temperature change is measured relative to the observation-based estimate of global temperature in 1990, instead of the modeled estimate of 1990 temperature. In this study, the energy balance model is forced to match the observation-based estimate of global temperature through 1999, whereas the IPCC TAR analysis gives past global temperatures based on an energy balance model with a scenario of past radiative forcing (since past radiative forcing from, e.g., aerosols is highly uncertain). This difference in methodology adds to a wider range of temperature change in this study than in the IPCC TAR.

4.3. Analysis of Stabilization of CO_2 Concentration

[57] In this section, we estimate the emission rates of CO_2 that arrive at constant CO_2 concentration levels following the set of five different CO_2 concentration trajectories, defined by *Wigley et al.* [1996], and shown in Figure 9a. These trajectories were designed to follow CO_2 concentration consistent with the IS92a emission scenario beginning

Figure 9. (opposite) Projections of CO_2 emissions and global average near-surface temperature driven by specified concentrations pathways (a) leading to constant CO_2 concentrations ranging from 450 to 1000 ppm specified by *Wigley et al.* [1996]. Estimates of (b) anthropogenic (i.e., fossil plus land use) CO_2 emissions, and (c) global average near-surface temperature anomaly deduced from specified concentrations pathways are shown by the solid curves for the reference parameterization of ISAM. Temperature is given as an anomaly from mid-1800s (see section 4.3 and Figure 6). The highest and lowest projections (low and high parameterizations of ISAM for emissions, and high and low parameterizations for temperature) are shown by the shaded area for only the pathway leading to stabilization at 550 ppm, and for all five pathways by the dashed curves. Prior to 2000, observation-based estimates of (Figure 9a) CO_2 concentrations, (Figure 9b) fossil CO_2 emissions, and (Figure 9c) temperature anomaly are shown by the circles.

in 1990, and branching off to reach constant CO_2 concentrations of 450, 550, 650, 750, or 1000 ppm over the following centuries [*Wigley et al.*, 1996]. Justification for various alternative time trajectories, stabilization levels, and related emissions, have been considered in detail in the IPCC TAR [*Morita et al.*, 2001] requiring assessment of a range of socio-economic factors corresponding to future emission scenarios. This section is concerned with the estimation of "anthropogenic" (i.e., the sum of CO_2 emissions resulting from fossil carbon and land use) emissions given specific CO_2 concentration trajectories, which is fundamentally a natural science question.

[58] The three alternative parameterizations (reference, low CO_2, and high CO_2) of the ISAM model are used to calculate the ocean and terrestrial CO_2 uptake resulting from the prescribed changes in CO_2 concentration. As in the emission scenario analyses in sections 4.1.2, observation-based global temperature and CO_2 are specified through 1999. From 2000 onward, global temperature is calculated from CO_2 radiative forcing only. The effects of aerosols and other greenhouse gases are neglected in these calculations since these roughly cancel each other (on a global scale) in the IS92a scenario up to 2100, and scenarios have not been associated with these CO_2 trajectories after 2100. The alternative parameterizations yield a range of climate projections. With CO_2 and global temperature defined in this way the ocean and terrestrial carbon cycle model components are also uncoupled from each other and can be calculated independently for the three alternative parameterizations. Note that in these cases, land use emissions are specified to follow the IS92a scenario until 2100, and are assumed to be zero thereafter. From the carbon budget, fossil emissions are equated to the calculated accumulation rate of carbon in the atmosphere, oceans, plus the terrestrial biosphere (including land use emissions).

[59] The results of these calculations are given in Table 3 and Figure 9. As with results for the emission scenarios in sections 4.1 and 4.2, results for the reference parameterization are not substantially different than those reported in the IPCC SAR [*Schimel et al.*, 1996], which were calculated with the Bern model [*Siegenthaler and Joos*, 1992]. Again the range of ISAM results, in this case anthropogenic CO_2 emissions, for the alternative parameterizations is wider than the range presented in the IPCC SRRF [*Schimel et al.*, 1995] but narrower than the results presented in the IPCC TAR using the *Joos et al.*'s [2001] model. For example, the ranges of anthropogenic emissions for the CO_2 trajectories leading to 450 and 1000 ppm overlap until 2040.

[60] Table 3 shows the modeled carbon budgets based on the different ISAM parameterizations applied to the stabilization CO_2 trajectories. Changes in carbon stocks of plants and soils, the oceans, the atmosphere, and fossil carbon are aggregated over each of the next three centuries. Since the change in atmospheric CO_2 is specified, the change in atmospheric carbon content is independent of the model parameterization. Once a constant CO_2 concentration is reached (see Figure 9a), the change in atmospheric carbon stock becomes zero. Note that the low CO_2 ISAM parameterization corresponds to the high extreme of the increase in plant and soil, and ocean carbon stocks along with the greatest decrease in fossil carbon stocks; the converse is the case for the high CO_2 ISAM parameterization while the reference case lies in between. Over the period from 2000 to 2099 inclusive, increase in carbon stocks by the oceans is larger than, but of comparable magnitude to, that of plants and soils. The range of carbon accumulation in plants and soils is, however, somewhat wider than that of the oceans accounting for the majority of the range of deduced fossil fuel emissions. Over the next two centuries, this pattern changes. Over the period from 2200 to 2299, increase in carbon stocks by the oceans is far larger than that of plants and soils, which in some cases is negative (a net source of CO_2). Furthermore,

Table 3. Carbon Budgets Over the Next Three Centuries for CO_2 Stabilization

	Carbon Stock Change Over Budget Period, Gt C					
Budget Period	Stabilization Level, ppm	Atm.		Ocean	Plants and Soils[a]	Fossil[b]
2000–2099	450	176.2	ref.	222.0	86.8	−485.0
			low	274.5	230.9	−681.7
			high	157.0	18.5	−351.7
	550	367.6	ref.	297.7	154.7	−820.0
			low	360.1	350.4	−1078.2
			high	220.7	63.8	−652.2
	650	497.1	ref.	334.9	188.8	−1020.8
			low	401.5	409.7	−1308.3
			high	252.7	87.2	−837.1
	750	573.2	ref.	353.1	205.8	−1132.2
			low	421.8	438.9	−1433.9
			high	268.7	99.0	−940.9
	1000	650.4	ref.	368.5	220.2	−1239.1
			low	438.5	463.3	−1552.3
			high	264.8	126.6	−1041.9
2100–2199	450	0.0	ref.	130.4	29.2	−159.6
			low	183.1	73.5	−256.6
			high	67.1	−0.5	−66.6
	550	20.8	ref.	202.6	62.4	−285.8
			low	276.5	144.1	−441.4
			high	113.4	11.5	−145.7
	650	103.6	ref.	269.2	104.8	−477.6
			low	358.5	226.4	−688.6
			high	161.3	33.2	−298.0
	750	225.8	ref.	321.5	143.3	−690.5
			low	421.1	298.0	−944.9
			high	201.2	55.1	−482.1
	1000	504.0	ref.	397.5	205.3	−1106.8
			low	509.9	409.9	−1423.8
			high	158.3	−0.4	−662.0
2200–2299	450	0.0	ref.	101.4	13.5	−114.9
			low	150.0	36.6	−186.6
			high	44.4	−3.3	−41.1
	550	0.0	ref.	148.5	20.5	−169.0
			low	217.3	56.9	−274.3
			high	67.7	−5.8	−61.9
	650	0.0	ref.	189.8	28.1	−217.9
			low	274.8	78.9	−353.8
			high	89.6	−8.0	−81.6
	750	14.0	ref.	229.5	40.7	−284.2
			low	327.9	109.2	−451.1
			high	113.4	−6.6	−120.8
	1000	167.8	ref.	313.2	82.7	−563.7
			low	433.7	196.8	−798.3
			high	170.7	9.4	−347.9

[a]Plant and soil stock change includes contribution from changing land use of −68.2 Gt C over 2000–2099, and zero over the later periods.

[b]Deduced decrease in fossil stocks equals net increase in atmosphere, ocean, and plant and soil stocks.

the range of carbon accumulation (caused by different model parameterizations) in plants and soils decreases in relation to that of the oceans.

[61] One artifact of these cases is that the range of land use emission prior to year 2000 does not match that specified exactly in scenario IS92a, and the CO_2 concentration trajectories (Figure 9a) were constructed with a different carbon cycle model.

[62] Consequently, the estimated fossil emissions following 1999 are discontinuous with the observation-based estimate of fossil emissions in 1999. In Figure 9b and in the IPCC TAR [*Prentice et al.*, 2001] anthropogenic CO_2 emissions are presented obscuring this artifact. Further consideration of appropriate ways of including uncertain land use emissions in CO_2 stabilization studies is needed to address this artifact [cf. *Bolin and Kheshgi*, 2001].

[63] Temperature anomaly is calculated from the prescribed CO_2 stabilization trajectories (Figure 9c). The range in temperature projections for a given CO_2 stabilization trajectory in this analysis depends primarily on the climate sensitivity ΔT_{2x}. The temperature range for a CO_2 stabilization trajectory, e.g., stabilizing at 550 ppm as shown in Figure 9c, is comparable in width to the range of reference temperature projections over the span of stabilization levels, i.e., 450–1000 ppm.

[64] We note that the calibration of ISAM was carried out in section 3 only for a scenario lasting one century, not the longer period considered for the stabilization of CO_2 concentration. Furthermore, interactions between ocean circulation/mixing and climate were not included, and these do become an important factor in slowing the ocean uptake of CO_2 after about 2050 in model studies [*Sarmiento et al.*, 1998; *Joos et al.*, 1999; *Prentice et al.*, 2001], although they have yet to be included in scenario analyses and the integrated assessment of climate change. Therefore the information contained in the model intercomparisons that are the basis for this use of ISAM may be insufficient in this respect for the analysis of stabilization of CO_2, which spans several centuries.

5. Concluding Discussion

5.1. Key Results

[65] (1) Trends in DGVM CO_2 uptake, and their dependence on CO_2 and temperature, are simulated by ISAM (see section 2.1). DGVMs exhibit a decrease in CO_2 uptake in response to a warming climate scenario. However, DGVMs exhibit a stronger increase in CO_2 uptake in response to enhanced CO_2 levels than assessed in the IPCC SAR [*Schimel et al.*, 1996]. The range of CO_2 fertilization effect exhibited by the DGVMs (Figures 3 and 4) is simulated with ISAM by calibrating ISAM's β-factor parameter to range from 0.35 to 0.9; this compares to a value of 0.39 used in ISAM for results for the IPCC SAR. A stronger CO_2 fertilization effect is in contrast to analyses [e.g., *Mooney et al.*, 1999] based on a growing quantity of data on plant and soil exposure to elevated CO_2 [e.g., *Curtis and Wang*, 1998]. Appropriate use of such experimental data in construction of global vegetation models is recommended [cf. *Luo and Reynolds*, 1999].

[66] (2) Detailed ocean models continue to exhibit a range of CO_2 uptake response to enhanced CO_2 levels (Figure 5), which is comparable to the IPCC SAR [*Schimel et al.*, 1996]. This range of ocean model behavior is simulated by ISAM and the effect of temperature on CO_2 solubility is included (see section 2.2). Little climate effect via circulation change, not accounted for in ISAM, is found [*Prentice et al.*, 2001] in model projections out to 2050.

[67] (3) Model reconstruction of CO_2 ocean uptake over the 1980s and 1990s (see section 3), when forced by the observed warming which is strong over these decades, gives an ocean uptake that is about 0.3 Gt C/yr lower than without the temperature effect on CO_2 solubility, as was done in the IPCC SAR [*Schimel et al.*, 1996] and the IPCC Special Report on Land Use, Land Use Change, and Forestry [*Bolin et al.*, 2000].

[68] (4) Observed terrestrial carbon uptake over a single decade is found to be of limited use in the calibration of terrestrial carbon cycle models until the potentially strong decadal variability in terrestrial CO_2 uptake is understood (see section 2.2).

[69] (5) Model-based carbon budgets over the past century match observation-based budgets of ocean CO_2 uptake and land use emissions (see section 3).

[70] (6) In the benchmark future emission scenario IS92a (see section 4.1), the modeled climate feedback compensates for a stronger CO_2 fertilization effect resulting in nearly identical projections, in the reference case, as in the IPCC SAR [*Schimel et al.*, 1996]. The range of ISAM results, however, is 640–804 ppm in 2100: a wider range than considered in past assessments [*Schimel et al.*, 1995].

[71] (7) The range of CO_2 projections (see section 4.2) found for the IPCC SRES emission scenarios is primarily due to the range of emission rates for the alternate scenarios, and secondarily to the range of modeled carbon cycle response. The consequent range of global temperature projections is wider than that highlighted by the *IPCC* [2001b], although probabilities are not assigned to this range [cf. *Wigley and Raper*, 2001]. The range of projected global temperature increase (Figure 8c) is primarily due to the range of Earth system response (i.e., the combined range of climate and carbon cycle response to an emission scenario) and secondarily to the range of emission scenarios.

[72] (8) Model projections of CO_2 emissions leading to stable CO_2 concentrations (see section 4.3) show ranges of anthropogenic CO_2 emissions that overlap with the emission pathways leading to different CO_2 concentration levels: for example, the range of anthropogenic (fossil plus land use) CO_2 emissions leading to 550 ppm overlaps with those leading to 450 and 650 ppm (see Figure 9b). Furthermore, since uncertainty in future land use emissions is not accounted for in this calculation, the range of deduced fossil fuel emissions must be wider than that for anthropogenic emissions. Ranges of model projections of global temperature are considerably broader: for example, the range of temperature change projected for the CO_2 trajectory leading to 550 ppm overlaps with the reference temperature projections for all cases studied (450–1000 ppm) over the next century and beyond (see Figure 9c). Moreover,

since the uncertainty in other climate forcing factors (e.g., other greenhouse gases and aerosols) has been neglected, accounting for these factors would result in an even wider range.

5.2. Methodology

[73] The accuracy of projections of future climate change is the central assessment question for the science of climate change. Assessments of climate change carried out by the IPCC have primarily used ranges of model results as a ''measure'' of the uncertainty of projections, given scenarios for human activities. Our interpretation of this measure is that: ''The envelope of alternative model simulations, if plausible responses, must be contained within the uncertainty range; in this way model intercomparisons form a lower-bound estimate of uncertainty range of future response.'' This approach has characteristics that we consider below in relation to the results presented in this paper:

[74] 1. Including ranges of behavior of additional components of the climate system increases the range of results for the coupled Earth system: In this study, we used a simple Earth system model to simulate the behavior of the ocean and terrestrial carbon cycles, and the climate system and to compute ranges of behavior of the integrated system. Including ranges of model results for each component increases the range of integrated system. For example, in the IPCC SRRF [*Schimel et al.*, 1995] and SAR [*Schimel et al.*, 1996] for CO_2 projections, the effects of changing climate on carbon cycle were not included; this is a partial cause for the narrower ranges of CO_2 projections seen in those assessments compared to the IPCC TAR [*Prentice et al.*, 2001]. Including the range of the modeled carbon cycle response increases the range of projected global temperature to be even wider than that communicated by the IPCC TAR. Further contributors to uncertainty neglected include uncertainty in: the response and effects of soil moisture, precipitation and humidity; aerosol and non-CO_2 radiative climate forcing; natural climate forcing factors; changes in ocean transport; effects of nitrogen fertilization of plants and soils; and interactions with land use beyond that accounted for in land use emission scenarios. Including these factors would further increase the range of integrated system results.

[75] 2. Including outlying models in the set of models that define a range of projections increases the range: Beyond the range of carbon cycle and climate model results represented by ISAM in this study, additional results have appeared. For example, *Cox et al.* [2000] find that a variant of the TRIFFID (a DGVM model), when combined with a different climate model and climate drivers (no aerosols) than prescribed by *Cramer et al.* [2001], led to considerably less accumulation of carbon in soils than contained in the range of ISAM results. This might be an artifact of the way ISAM was parameterized to match the range of DGVMs given the limited information on modeled mechanisms for the behavior of the simulations. Nevertheless, if the *Cox et al.*'s [2000] simulation were spanned by the ISAM range, the range of projections would extend to even higher temperatures and CO_2 concentrations. On the other hand, if the mechanism for interactions between cirrus clouds and climate as proposed by *Lindzen et al.* [2001] were included, then the range of climate sensitivity would be extended to lower values and the range of projections would extend to even lower temperatures and CO_2 concentrations. Since model intercomparisons will not include all plausible responses of the system, their range may underestimate uncertainty.

[76] 3. Tests for plausibility of component models in intercomparisons: If model results are found to be implausible, then they need not be considered in the range for modeling the integrated system. However, the grounds for inclusion of model results in model intercomparisons, and their use in defining assessed ranges of behavior, is often not transparent, and may be restrictive in terms of their model structure (e.g., using only DGVM results in this study). Transparent grounds for model consideration and rejection are needed.

[77] 4. Observational constraints on integrated system results: Past behavior of the Earth system does provide constraints on the range of the integrated system response. For example, in an earlier study using ISAM [*Kheshgi et al.*, 1999; *Kheshgi and Jain*, 2000], observational constraints were used to estimate a range of Earth system model parameters. Ranges of model parameters generated from model intercomparisons could, in principle, be used to define prior ranges of model parameters. Bayesian statistical estimation could then be used to apply observational constraints. There are many aspects of this kind of analysis that would need to be addressed: e.g., characterization and inclusion of variability in both climate and carbon cycle, observational uncertainties, all relevant factors in past climate change, and model structure effects on the relationship between past and future model behavior. Clearly, further work is needed to apply observational constraints on the integrated system in an appropriate manner. Nevertheless, observational constraints do hold some potential for limiting uncertainty in projections [cf. *Tol and De Vos*, 1998; *Forest et al.*, 2002].

[78] 5. Assignment of probability to ranges of projections: Many of the issues in the use of model intercomparisons for the estimation of uncertainty in projections could be avoided if it were possible to assign probabilities to each alternate model response, that is the probability that a response is the ''true'' outcome. The high profile result of the IPCC TAR [*IPCC*, 2001b] was a higher range of projected global temperature increase over the next century (1.4°–5.8°C) than was assessed in the IPCC SAR [*IPCC*, 1996], 1.0°–3.5°C (cf. projections in section 4.2). However, no probability was assigned in the IPCC TAR to this range, bringing into question the usefulness of this range in characterizing the risk of global climate change [*Reilly et al.*, 2001; *Schneider*, 2001; *Wigley and Raper*, 2001] and our ability to assign probabilities [*Allen et al.*, 2001; *Grubler and Nakicenovic*, 2001]. Doing so remains a highly subjective exercise [*Morgan and Keith*, 1995]. In studies [*Schneider*, 2001; *Wigley and Raper*, 2001] where probabilities were assigned to alternative emission scenarios and models, a narrow probability distribution was found partially due to the specification that these factors are statistically independent. Furthermore, *Wigley and Raper* [2001] found that their modeled uncertainty in their carbon cycle

response had negligible effects on their resulting temperature uncertainty. This is in contrast to the increased range of temperature projections found in section 4.2 caused, in part, by the range of carbon cycle response. These, of course, are different measures of uncertainty. We note that *Wigley and Raper*'s [2001] conclusion depends on the assumed probability distributions of carbon cycle and climate response and the correlation between these probability distributions, which depends on the strength of modeled climate effects on carbon cycle [cf. *Cubasch et al.*, 2001]. The strength of the climate feedback on carbon cycle, and the corresponding correlation between climate and CO_2, continues to differ considerably between studies [e.g., *Cox et al.*, 2000; *Friedlingstein et al.*, 2001] and we do not know which is likely to be true.

[79] **Acknowledgments.** We wish to acknowledge Martin Heimann, Colin Prentice, and Corinne Le Quéré for suggestions and facilitation of the acquisition of model intercomparison results. We acknowledge Wolfgang Cramer, Jim Orr, and the many contributors of results to the model intercomparison projects. Also, we acknowledge Fortunat Joos for providing radiative forcing contributions from non-CO_2 greenhouse gases and aerosols as used in the IPCC TAR. The modeling studies were supported in part by the Integrated Assessment program, Biological and Environmental Research (BER), U.S. Department of Energy (DOE-DE-FG02-01ER63069).

References

Allen, M., S. C. B. Raper, and J. Mitchell, Uncertainty in the IPCC's third assessment report, *Science*, *293*, 430–433, 2001.

Bolin, B., and H. S. Kheshgi, On strategies for reducing greenhouse gas emissions, *Proc. Natl. Acad. Sci. U.S.A.*, *98*, 4850–4854, 2001.

Bolin, B., R. Sukumar, P. Ciais, W. Cramer, P. Jarvis, H. Kheshgi, C. Nobre, S. Semenov, and W. Steffen, Global perspective, in *Land Use, Land-Use Change, and Forestry: A Special Report of the Intergovernmental Panel on Climate Change*, edited by R. T. Watson, et al., pp. 23–51, Cambridge Univ. Press, New York, 2000.

Bretherton, F. P., K. Bryan, and J. D. Woods, Time-dependent greenhouse-gas-induced climate change, in *Climate Change: The IPCC Scientific Assessment*, edited by J. T. Houghton, G. J. Jenkins, and J. J. Ephraums, pp. 173–194, Cambridge Univ. Press, New York, 1990.

British Petroleum Company, *BP Statistical Review of World Energy 1999*, Br. Pet. Co., London, 2000.

Brovkin, V., A. Ganopolski, and Y. Svirezhev, A continuous climate-vegetation classification for use in climate-biosphere studies, *Ecol. Modell.*, *101*, 251–261, 1997.

Cox, P. M., R. A. Betts, C. D. Jones, S. A. Spall, and I. A. Toterdell, Acceleration of global warming due to carbon-cycle feedbacks in a coupled climate model, *Nature*, *408*, 184–187, 2000.

Cramer, W., D. W. Kicklighter, A. Bondeau, B. Moore III, G. Churkina, B. Nemry, A. Ruimy, and A. L. Schloss, Comparing global models of terrestrial net primary productivity (NPP): Overview and key results, *Global Change Biol.*, *5*, 1–15 suppl. 1, 1999.

Cramer, W., et al., Global response of terrestrial ecosystem structure and function to CO_2 and climate change: Results from six dynamic global vegetation models, *Global Change Biol.*, *7*, 357–374, 2001.

Cubasch, U., G. A. Meehl, G. J. Boer, R. J. Stouffer, M. Dix, A. Noda, C. A. Senior, S. Raper, and K. S. Yap, Projections of future climate change, in *Climate Change 2001: The Scientific Basis: Contribution of WGI to the Third Assessment Report of the IPCC*, edited by J. T. Houghton et al., pp. 525–582, Cambridge Univ. Press, New York, 2001.

Curtis, P. S., and X. Wang, A meta-analysis of elevated CO_2 effects on woody plant mass, form and physiology, *Oecologia*, *113*, 299–313, 1998.

DeFries, R. S., C. B. Field, I. Fung, G. J. Collatz, and L. Bounoua, Combining satellite data and biogeochemical models to estimate global effects of human-induced land cover change on carbon emissions and primary productivity, *Global Biogeochem. Cycles*, *13*, 803–815, 1999.

Enting, I. G., , T. M. L. Wigley, and M. Heimann (Eds.), Future emissions and concentrations of carbon dioxide: Key ocean/atmosphere/land analyses, *CSIRO Div. of Atmos. Res. Tech. Pap. 31*, CSIRO, Australia, 1994.

Foley, J. A., I. C. Prentice, N. Ramankutty, S. Levis, D. Pollard, S. Sitch, and A. Haxeltine, An integrated biosphere model of land surface processes, terrestrial carbon balance, and vegetation dynamics, *Global Biogeochem. Cycles*, *10*, 603–628, 1996.

Forest, C. E., P. H. Stone, A. P. Sokolov, M. R. Allen, and M. D. Webster, Quantifying uncertainties in climate system properties with the use of recent climate observations, *Science*, *295*, 113–117, 2002.

Friedlingstein, P., L. Bopp, P. Ciais, J.-L. Dufresne, L. Fairhead, and H. LeTreut, Positive feedback between future climate change and the carbon cycle, *Geophys. Res. Lett.*, *28*, 1543–1546, 2001.

Friend, A. D., A. K. Stevens, R. G. Knox, and M. G. R. Cannell, A process-based, terrestrial biosphere model of ecosystem dynamics (Hybrid v3.0), *Ecol. Modell.*, *95*, 249–287, 1997.

Gruber, N., J. L. Sarmiento, and T. F. Stocker, An improved method for detecting anthropogenic CO_2 in the Oceans, *Global Biogeochem. Cycles*, *10*, 809–837, 1996.

Grubler, A., and N. Nakicenovic, Identifying dangers in an uncertain climate, *Nature*, *412*, 15, 2001.

Harvey, L. D. D., Effect of model structure on the response of terrestrial biosphere models to CO_2 and temperature increases, *Global Biogeochem. Cycles*, *3*, 137–153, 1989a.

Harvey, L. D. D., Managing atmospheric CO_2, *Clim. Change*, *15*, 343–381, 1989b.

Harvey, L. D. D., J. Gregory, M. Hoffert, A. Jain, M. Lal, R. Leemans, S. C. B. Raper, T. M. L. Wigley, and de J. R. Wolde, *An Introduction to Simple Climate Models Used in the IPCC Second Assessment Report, IPCC Tech. Pap. II*, Intergovernmental Panel on Clim. Change, Bracknell, 1997.

Hoffert, M. I., A. J. Callegari, and C.-T. Hsieh, The role of deep sea heat storage in the secular response to climate forcing, *J. Geophys. Res.*, *85*, 6667–6679, 1980.

Houghton, R. A., The annual net flux of carbon to the atmosphere from changes in land use 1850–1990, *Tellus, Ser. B*, *50*, 298–313, 1999.

Houghton, R. A., A new estimate of global sources and sinks of carbon from land-use change (abstract), *Eos Trans. AGU*, *81*, Spring Meet. Suppl., S281, 2000.

Huntingford, C., P. M. Cox, and T. M. Lenton, Contrasting responses of a simple terrestrial ecosystem model to global change, *Ecol. Modell.*, *134*, 41–58, 2000.

Intergovernmental Panel on Climate Change (IPCC), *Climate Change 1995: The Science of Climate Change, Contribution of WGI to the Second Assessment Report of the Intergovernmental Panel on Climate Change*, Cambridge Univ. Press, New York, 1996.

Intergovernmental Panel on Climate Change (IPCC), *Revised 1996 IPCC Guidelines for National Greenhouse Gas Inventories. Reference Manual*, Geneva, 1997.

Intergovernmental Panel on Climate Change (IPCC), *Climate Change 2001: Synthesis Report of the IPCC Third Assessment Report*, Cambridge Univ. Press, New York, 2001a.

Intergovernmental Panel on Climate Change (IPCC), *Climate Change 2001: The Scientific Basis: Contribution of WGI to the Third Assessment Report of the IPCC*, Cambridge Univ. Press, New York, 2001b.

Jain, A., and K. Hayhoe, Global air pollution problems, in *Handbook of Atmospheric Sciences*, edited by C. N. Hewitt and A. V. Jackson, pp. 339–371, Blackwell Sci., Malden, Mass., 2003.

Jain, A. K., H. S. Kheshgi, and D. J. Wuebbles, Integrated science model for assessment of climate change, *Rep. 94-TP59.08*, Air and Waste Manage. Assoc., Pittsburgh, Pa., 1994.

Jain, A. K., H. S. Kheshgi, M. I. Hoffert, and D. J. Wuebbles, Distribution of radiocarbon as a test of global carbon cycle models, *Global Biogeochem. Cycles*, *9*, 153–166, 1995.

Jain, A. K., H. S. Kheshgi, and D. J. Wuebbles, A globally aggregated reconstruction of cycles of carbon and its isotopes, *Tellus, Ser. B*, *48*, 583–600, 1996.

Jones, P. D., D. E. Parker, T. J. Osborn, and K. R. Briffa, Global and hemispheric temperature anomalies—Land and marine instrumental records, in *Trends: A Compendium of Data on Global Change*, Oak Ridge Natl. Lab., Oak Ridge, Tenn., 2000.

Joos, F., G.-K. Plattner, T. Stocker, O. Marchal, and A. Schmittner, Global warming and marine carbon cycle feedbacks on future atmospheric CO_2, *Science*, *284*, 464–467, 1999.

Joos, F., I. C. Prentice, S. Sitch, R. Meyer, G. Hooss, G.-K. Plattner, S. Gerber, and K. Hasselmann, Global warming feedbacks on terrestrial carbon uptake under the Intergovernmental Panel on Climate Change (IPCC) emission scenarios, *Global Biogeochem. Cycles*, *15*(4), 891–907, 2001.

Kattenburg, A., F. Giorgi, H. Grassl, G. A. Meehl, J. F. B. Mitchell, R. J. Stouffer, T. Tokioka, A. J. Weaver, and T. M. L. Wigley, Climate models-

Projections for future climate, in *Climate Change 1995: The Science of Climate Change: Contribution of WGI to the Second Assessment Report of the IPCC*, edited by J. T. Houghton et al., pp. 285–357, Cambridge Univ. Press, New York, 1996.

Keeling, C. D., The carbon dioxide cycle: Reservoir models to depict the exchange of atmospheric carbon dioxide with the oceans and land plants, in *Chemistry of the Lower Atmosphere*, edited by S. I. Rasool, pp. 251–329, Plenum, New York, 1973.

Keeling, C. D., and T. P. Whorf, Atmospheric CO_2 records from sites in the SIO air sampling network, in *Trends: A Compendium of Data on Global Change*, Carbon Dioxide Inf. Anal. Cent., Oak Ridge Natl. Lab., Oak Ridge, Tenn., 2000.

Kheshgi, H. S., and A. K. Jain, Uncertainty in projected CO_2 responses to future emission scenarios (abstract), *Eos Trans. AGU*, *81*, Spring Meet. Suppl., S17, 2000.

Kheshgi, H. S., and B. S. White, Modelling ocean carbon cycle with a nonlinear convolution model, *Tellus, Ser. B*, *48*, 3–12, 1996.

Kheshgi, H. S., A. K. Jain, and D. J. Wuebbles, Accounting for the missing carbon sink with the CO_2 fertilization effect, *Clim. Change*, *33*, 31–62, 1996.

Kheshgi, H. S., A. K. Jain, and D. J. Wuebbles, Model-based estimation of the global carbon budget and its uncertainty from carbon dioxide and carbon isotope records, *J. Geophys. Res.*, *104*, 31,127–31,144, 1999.

Leggett, J., W. J. Pepper, and R. J. Swart, Emission scenarios for the IPCC: An update, in *Climate Change 1992: The Supplementary Report to the IPCC Scientific Assessment*, edited by J. T. Houghton, B. A. Callander, and S. K. Varney, pp. 69–96, Cambridge Univ. Press, New York, 1992.

Le Quéré, C., et al., Two decades of ocean CO_2 sink and variability, paper presented at 6th International CO_2 Conference, Sendai, Japan, Oct. 1–5, 2001.

Lindzen, R. S., M.-D. Chou, and A. Y. Hou, Does the Earth have an infrared iris?, *Bull. Am. Meteorol. Soc.*, *82*, 417–432, 2001.

Luo, Y., and J. F. Reynolds, Validity of extrapolating field CO_2 experiments to predict carbon sequestration in natural ecosystems, *Ecology*, *80*, 1568–1583, 1999.

Marland, G., T. A. Boden, and R. J. Andres, Global, regional, and national CO_2 emissions, in *Trends: A Compendium of Data on Global Change*, Carbon Dioxide Inf. Anal. Cent., Oak Ridge Natl. Lab., U.S. Dep. of Energy, Oak Ridge, Tenn., 2000.

Mitchell, J. F. B., T. C. Johns, J. M. Gregory, and S. F. B. Tett, Climate response to increasing levels of greenhouse gases and sulphate aerosols, *Nature*, *376*, 501–504, 1995.

Mooney, H., J. Canadell, F. S. Chapin, J. Ehleringer, C. Korner, R. McMurtrie, W. Parton, L. Pitelka, and D. E. Schulze, Ecosystem physiology responses to global change, in *The Terrestrial Biosphere and Global Change*, edited by B. H. Walker et al., Cambridge Univ. Press, New York, 1999.

Morgan, M. G., and D. W. Keith, Subjective judgements by climate experts, *Environ. Sci. Technol.*, *29*, 468–476A, 1995.

Morita, T., et al., Greenhouse gas emission mitigation scenarios and implications, in *Climate Change 2001: Mitigation: Contribution of WGIII to the Third Assessment Report of the IPCC*, edited by B. Metz et al., pp. 115–166, Cambridge Univ. Press, New York, 2001.

Nakicenovic, N., et al., *IPCC Special Report on Emissions Scenarios*, Cambridge Univ. Press, New York, 2000.

Orr, J., et al., Estimates of anthropogenic carbon uptake from four 3-D global ocean models, *Global Biogeochem. Cycles*, *15*, 43–60, 2001.

Orr, J. C., and J.-C. Dutay, OCMIP mid-project workshop, *Res. GAIM Newsl.*, *3*, 4–5, 1999.

Prentice, C., G. Farquhar, M. Fasham, M. Goulden, M. Heimann, V. Jaramillo, H. Kheshgi, C. L. Quéré, R. Scholes, and D. Wallace, The carbon cycle and atmospheric CO_2, in *Climate Change 2001: The Scientific Basis: Contribution of WGI to the Third Assessment Report of the IPCC*, edited by J. T. Houghton et al., pp. 183–237, Cambridge Univ. Press, New York, 2001.

Ramaswamy, V., O. Boucher, J. Haigh, D. Hauglustaine, J. Haywood, G. Myhre, T. Nakajima, G. Y. Shi, and S. Solomon, Radiative forcing of climate change, in *Climate Change 2001: The Scientific Basis: Contribution of WGI to the Third Assessment Report of the IPCC*, edited by J. T. Houghton et al., pp. 349–416, Cambridge Univ. Press, New York, 2001.

Reilly, J., P. H. Stone, C. E. Forest, M. D. Webster, H. D. Jacoby, and R. G. Prinn, Uncertainty and climate change assessments, *Science*, *293*, 430–433, 2001.

Sarmiento, J. L., T. M. C. Hughes, R. J. Stouffer, and S. Manabe, Simulated response of the ocean carbon cycle to anthropogenic climate warming, *Nature*, *393*, 245–249, 1998.

Schimel, D., I. Enting, M. Heimann, T. Wigley, D. Raynaud, D. Alves, and U. Siegenthaler, CO_2 and the carbon cycle, in *Climate Change 1994: Radiative Forcing of Climate Change and an Evaluation of the IPCC IS92 Emission Scenarios*, edited by J. T. Houghton et al., pp. 35–71, Cambridge Univ. Press, New York, 1995.

Schimel, D., D. Alves, I. Enting, M. Heimann, F. Joos, D. Raynaud, and T. Wigley, CO_2 and the carbon cycle, in *Climate Change 1995: The Science of Climate Change: Contribution of WGI to the Second Assessment Report of the IPCC*, edited by J. T. Houghton et al., pp. 65–86, Cambridge Univ. Press, New York, 1996.

Schneider, S. H., What is "dangerous" climate change?, *Nature*, *411*, 17–19, 2001.

Schwartz, S. E., and M. O. Andreae, Uncertainty in climate change caused by aerosols, *Science*, *272*, 1121–1122, 1996.

Siegenthaler, U., and F. Joos, Use of a simple model for studying oceanic tracer distributions and the global carbon cycle, *Tellus, Ser. B*, *44*, 186–207, 1992.

Sitch, S., The role of vegetation dynamics in the control of atmospheric CO_2 content, Ph.D. thesis, Univ. of Lund, Sweden, 2000.

Tol, R. S. J., and A. F. De Vos, A Bayesian statistical analysis of the enhanced greenhouse effect, *Clim. Change*, *38*, 87–112, 1998.

Volk, T., and M. I. Hoffert, Ocean carbon pumps: Analysis of relative strengths and efficiencies in ocean-driven atmospheric CO_2 changes, in *Carbon Cycle and Atmospheric CO_2: Natural Variations Archean to Present*, edited by E. Sundquist and W. S. Broecker, pp. 91–110, AGU, Washington, D. C., 1985.

Watson, R. T., H. Rodhe, H. Oeschger, and U. Siegenthaler, Greenhouse gases and aerosols, in *Climate Change, The IPCC Scientific Assessment*, edited by J. T. Houghton, G. J. Jenkins, and J. J. Ephraums, pp. 1–40, Cambridge Univ. Press, Cambridge, 1990.

Wigley, T. M. L., Balancing the carbon budget. Implications for projections of future carbon dioxide concentration changes, *Tellus, Ser. B*, *45*, 409–425, 1993.

Wigley, T. M. L., *The Science of Climate Change: Global and U.S. Perspectives*, Pew Cent. on Global Clim. Change, Arlington, Va., 1999.

Wigley, T. M. L., and S. C. B. Raper, Interpretation of high projections for global-mean warming, *Science*, *293*, 451–454, 2001.

Wigley, T. M. L., R. Richels, and J. A. Edmonds, Economic and environmental choices in the stabilization of CO_2 concentrations: Choosing the "right" emissions pathway, *Nature*, *379*, 240–243, 1996.

Wigley, T. M. L., A. K. Jain, F. Joos, B. S. Nyenzi, and P. R. Shukla, *Implications of Proposed CO_2 Emissions Limitations, IPCC Tech. Pap. 4*, Intergovernmental Panel on Clim. Change, Bracknell, 1997.

Woodward, F. I., M. R. Lomas, and R. A. Betts, Vegetation-climate feedbacks in a greenhouse world, *Philos. Trans. R. Soc. London, Ser. B*, *353*, 29–38, 1998.

A. K. Jain, Department of Atmospheric Sciences, University of Illinois, Urbana, IL 61801, USA.

H. S. Kheshgi, Corporate Strategic Research, ExxonMobil Research and Engineering Company, Route 22E, Annandale, NJ 08801, USA. (haroon.s.kheshgi@exxonmobil.com)